Introduzione alle fibre ottiche

Edoardo Milotti

Corso di Fondamenti Fisici di Tecnologia Moderna

A. A. 2021-22

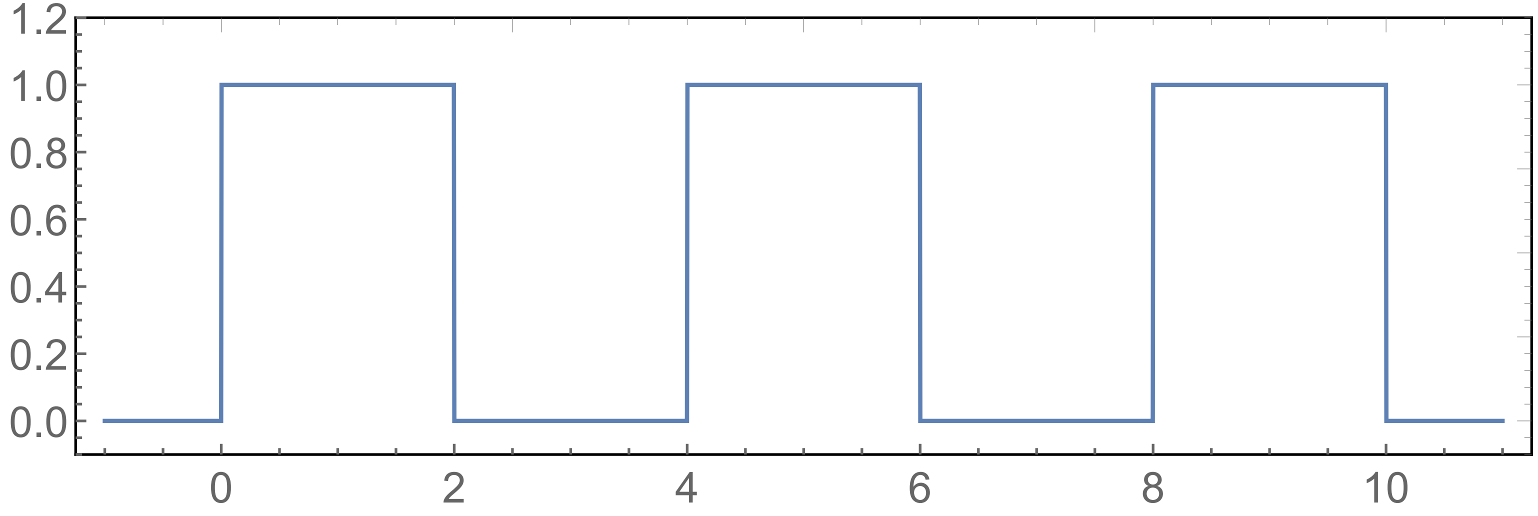

Bit rate basso
Larghezza di banda piccola

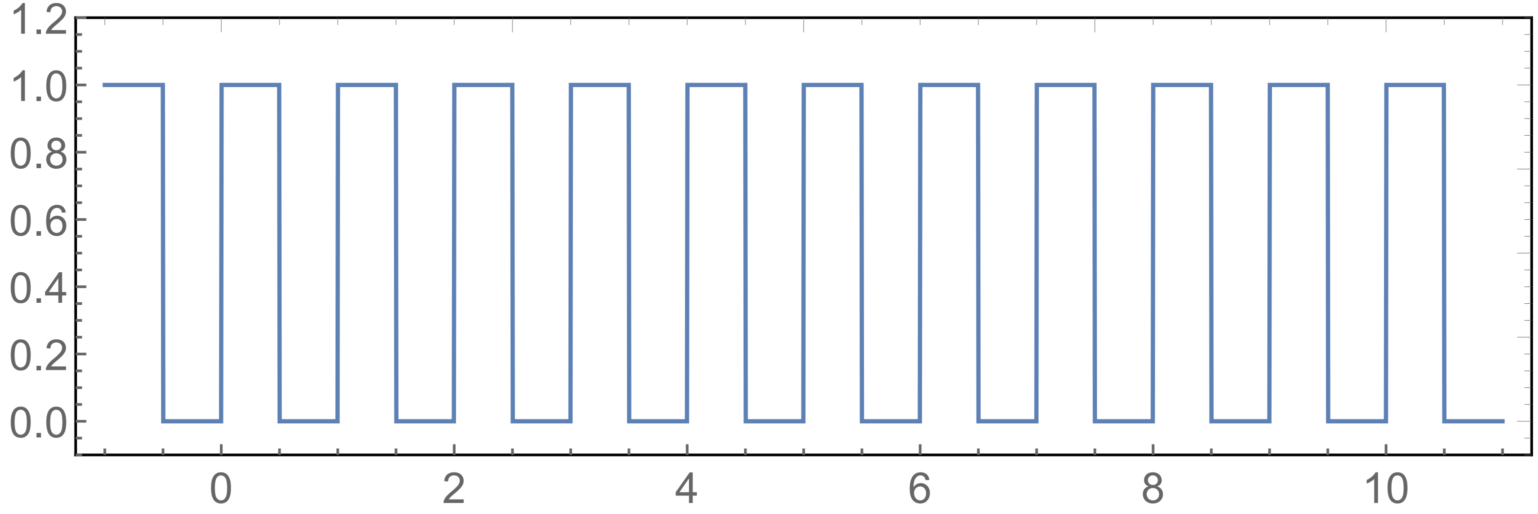

Bit rate alto
Larghezza di banda grande

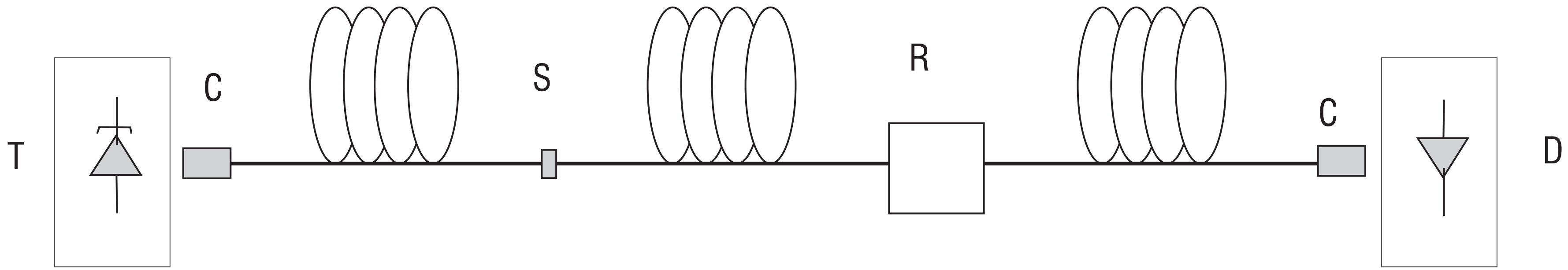

Figure 7-3 *A typical fiber optic communication system: T, transmitter; C, connector; S, splice; R, repeater; D, detector*

Le fibre ottiche permettono di stabilire canali di telecomunicazione a larga banda, grazie alla possibilità di trasmettere segnali con bassissima dispersione.

Riflessione totale: se $\frac{n_1}{n_2} > 1$ non tutti gli angoli di rifrazione sono possibili, infatti (dalla legge di Snell)

$$\sin\theta_2 = \frac{n_1}{n_2}\sin\theta_1$$

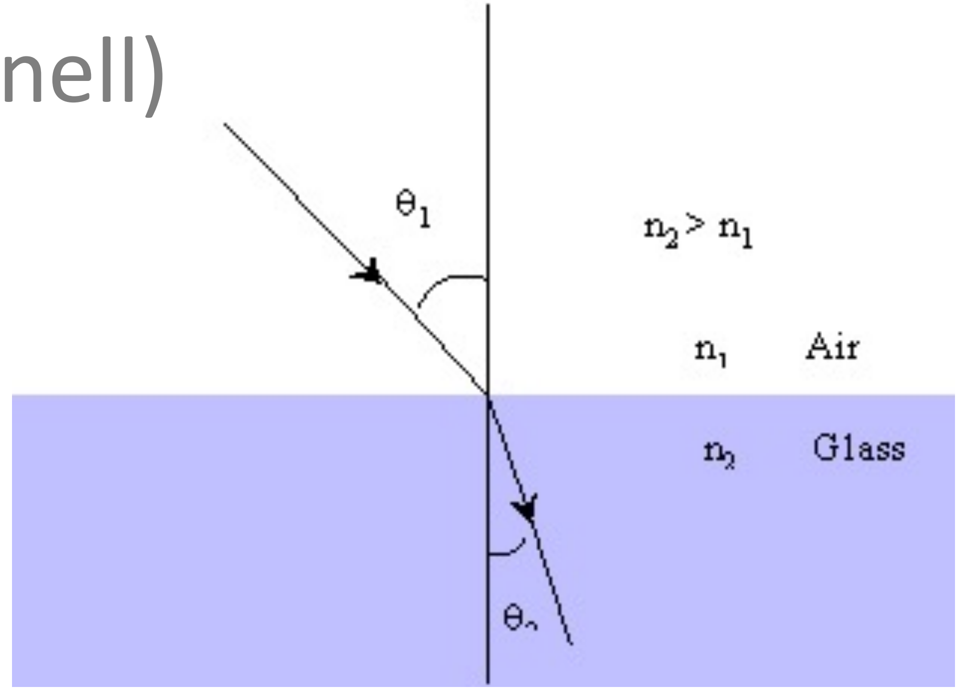

allora esiste un angolo limite tale che

$$\frac{n_1}{n_2}\sin\theta_1^{(\lim)} = 1 \quad \Rightarrow \quad \theta_1^{(\lim)} = \arcsin\frac{n_2}{n_1}$$

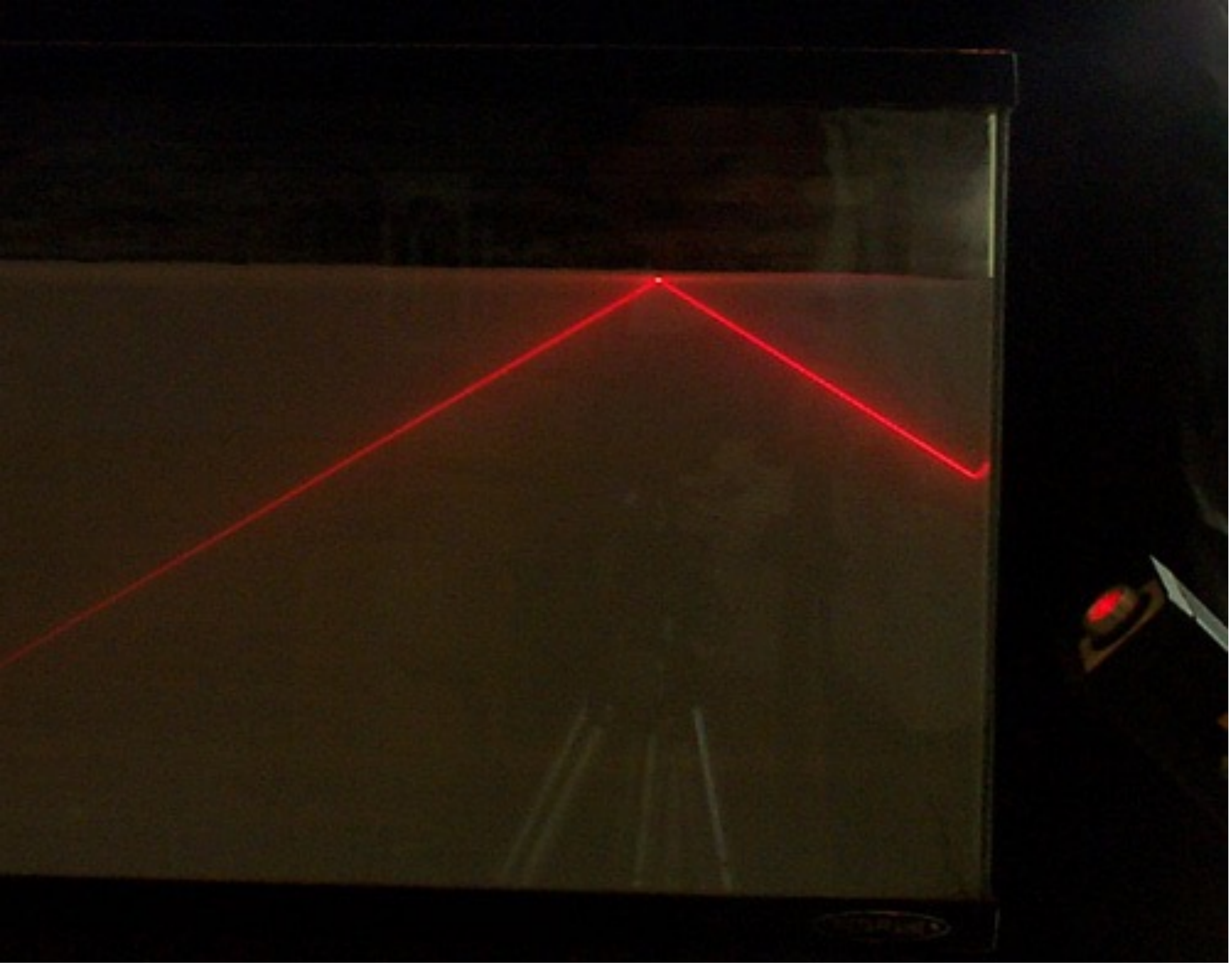

$$\theta_1^{(\lim)} = \arcsin \frac{n_2}{n_1}$$

nel caso dell’interfaccia aria-acqua
$n_1 \approx 1.33$,
$n_2 \approx 1$, allora

$$\theta_1^{(\lim)} \approx 48^\circ.75$$

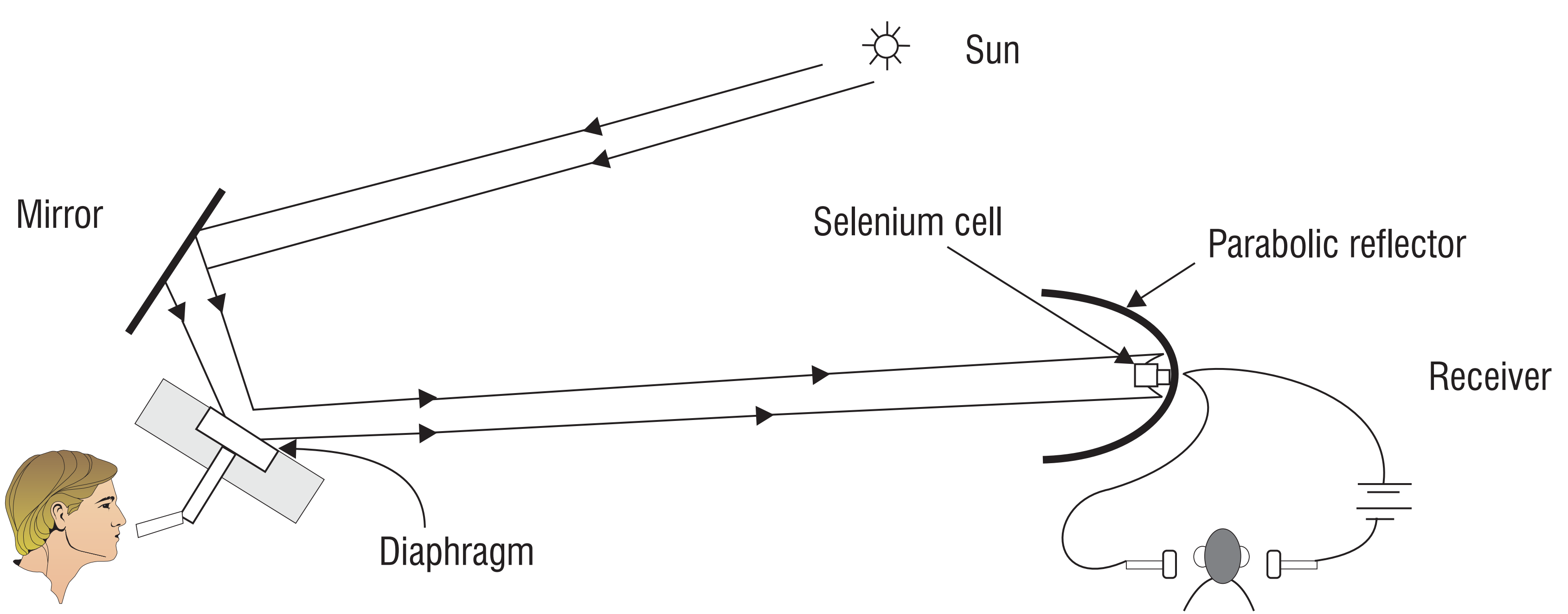

Figure 7-2 *Schematic of the photophone invented by Bell. In this system, sunlight was modulated by a vibrating diaphragm and transmitted through a distance of about 200 meters in air to a receiver containing a selenium cell connected to the earphone.*

vedi: Ghatak and Thyagarajan, "Optical Waveguides and Fibers", Fundamentals of Photonics, Module 1.7
https://spie.org/publications/fundamentals-of-photonics-modules

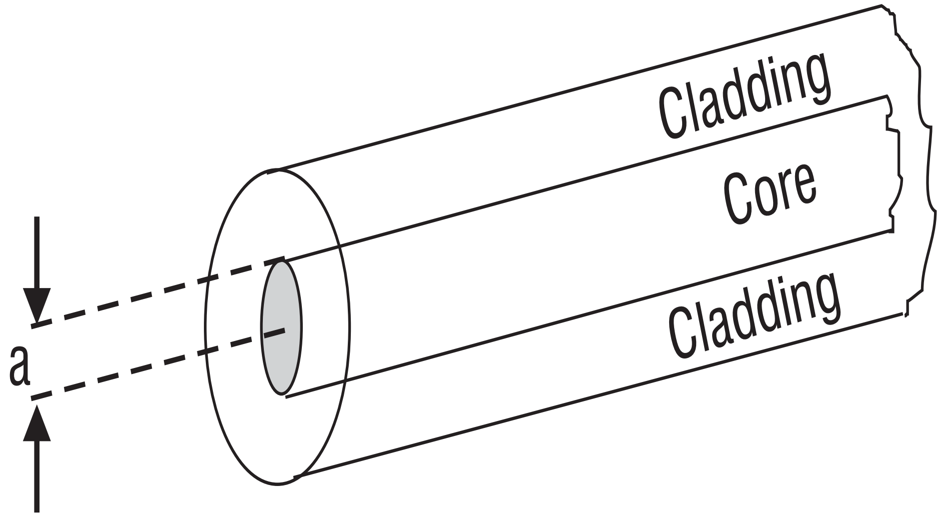

$$n = n_1 \quad \text{for} \quad r < a$$
$$n = n_2 \quad \text{for} \quad r > a$$

$$\Delta = \frac{n_1^2 - n_2^2}{2n_1^2}$$

$n_1 - n_2 \ll 1$

$$\Delta = \frac{(n_1 + n_2)(n_1 - n_2)}{2{n_1}^2} \approx \frac{(n_1 - n_2)}{n_1} \approx \frac{(n_1 - n_2)}{n_2}$$

(questo è un parametro importante per caratterizzare la fibra)

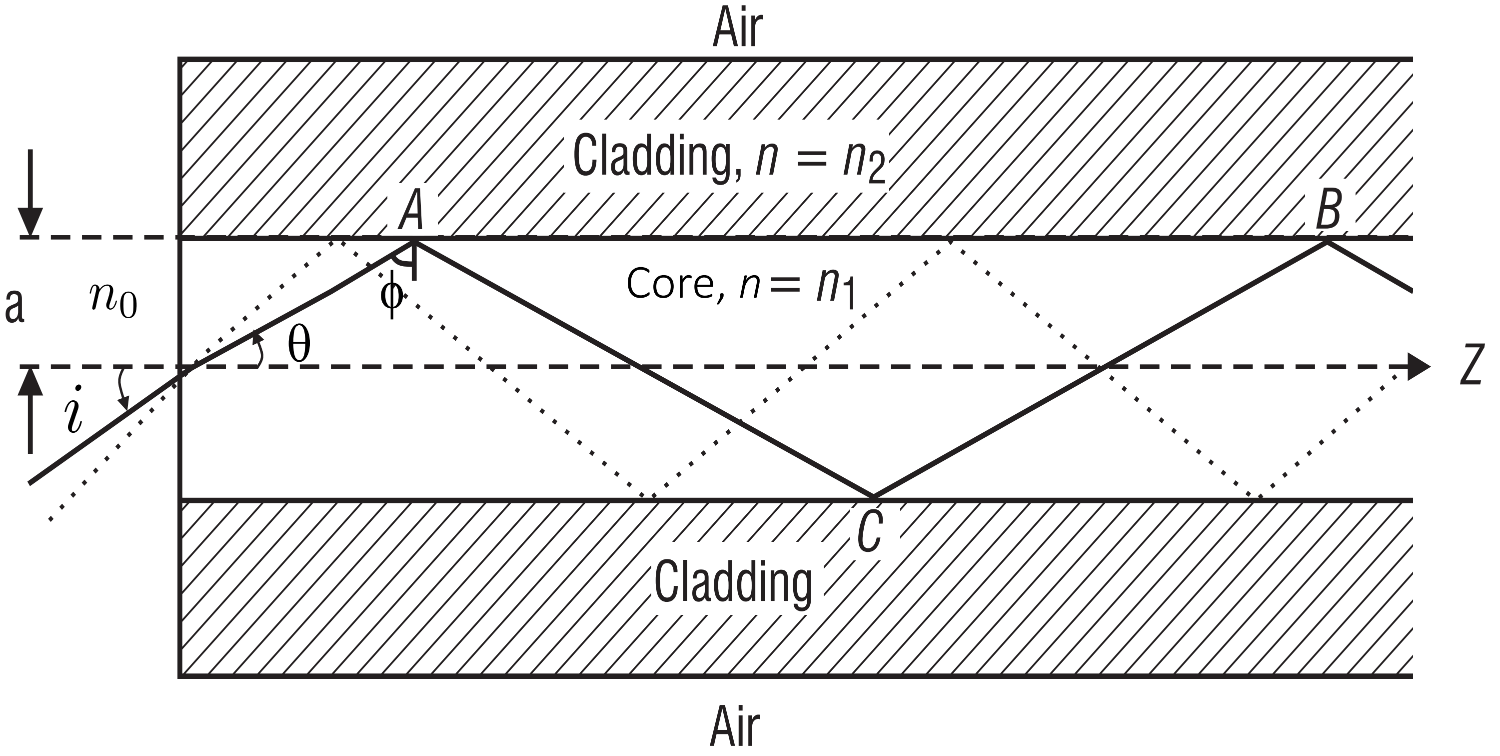

For a typical (multimode) fiber, $a \approx 25$ µm, $n_2 \approx 1.45$ (pure silica), and $\Delta \approx 0.01$, giving a core index of $n_1 \approx 1.465$. The cladding is usually pure silica while the core is usually silica doped with germanium. Doping by germanium results in a typical increase of refractive index from n_2 to n_1.

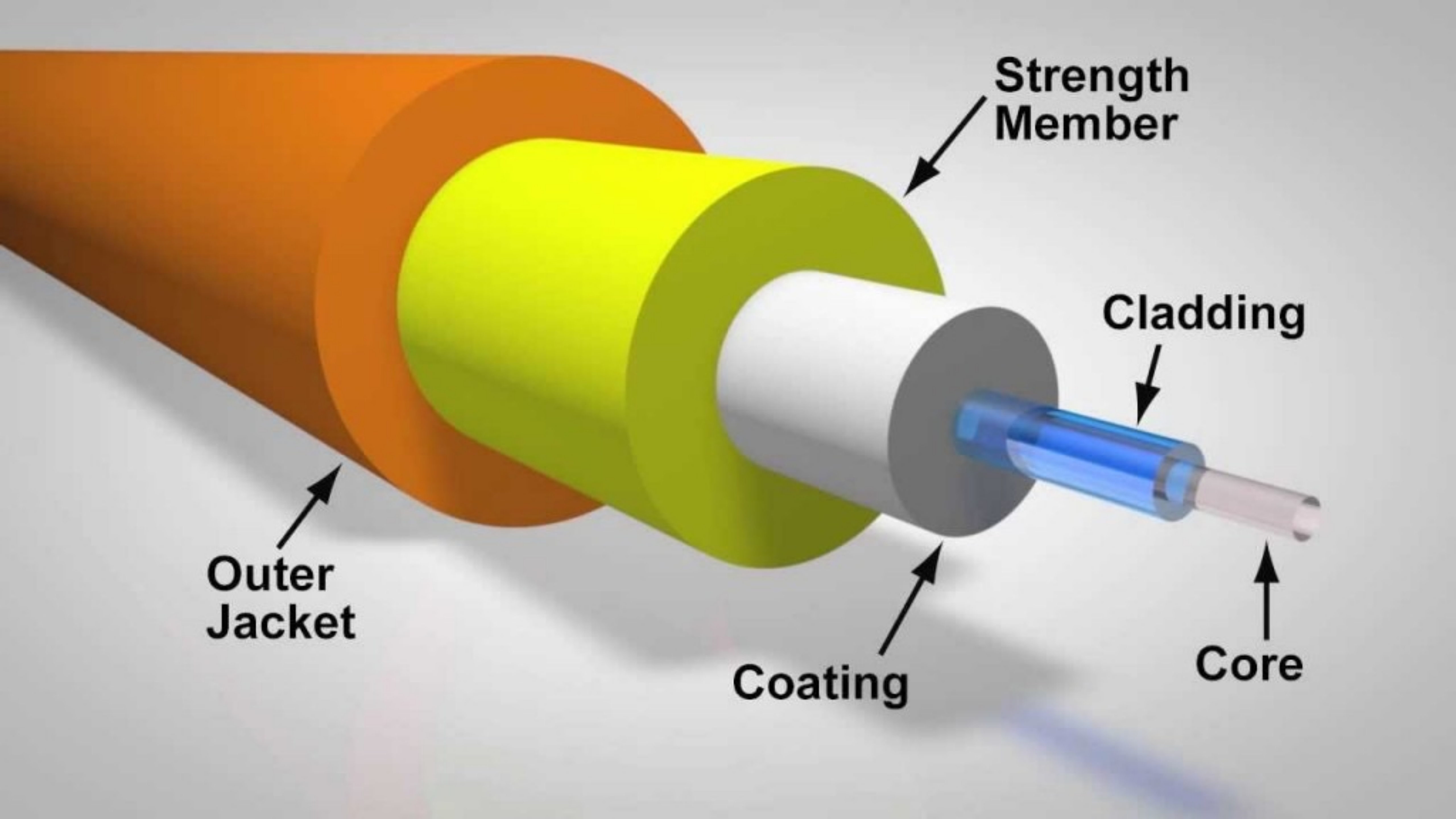
Strength
Member
Cladding
Outer
Jacket
Coating
Core

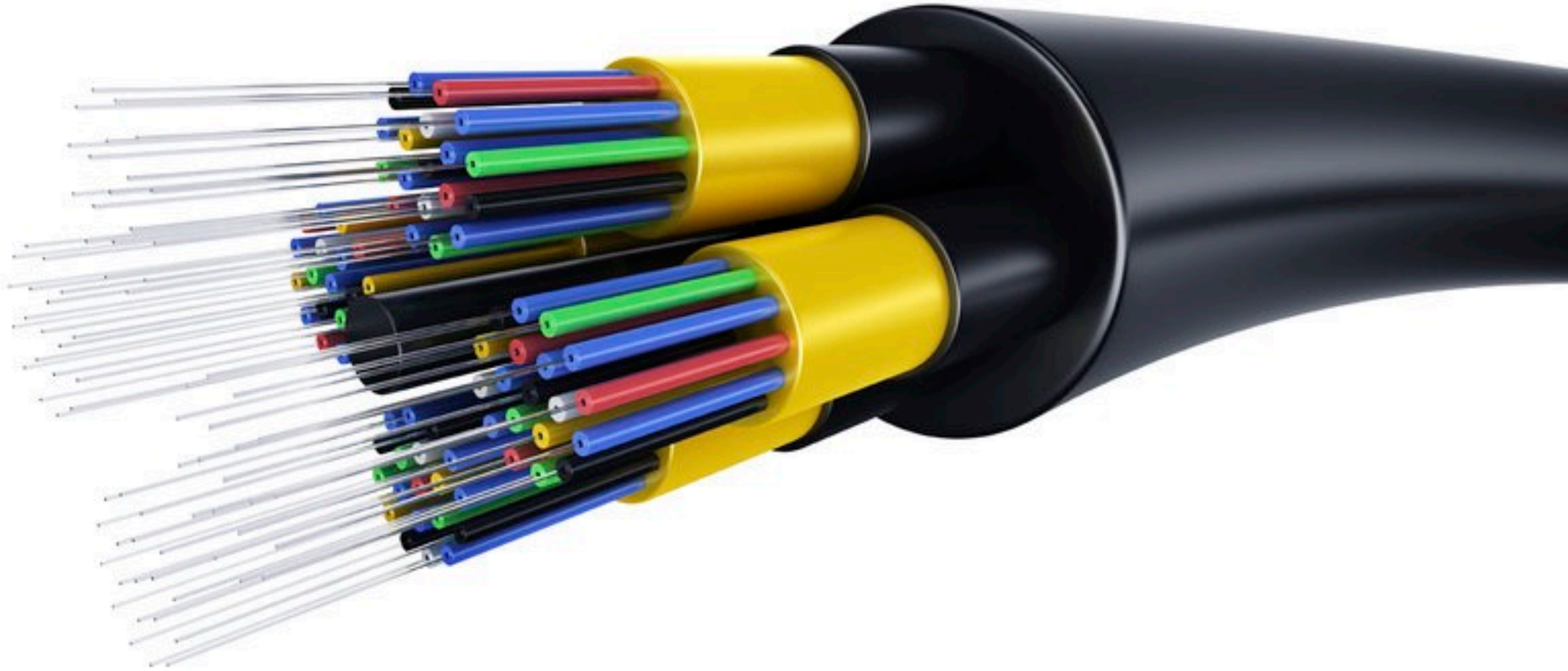

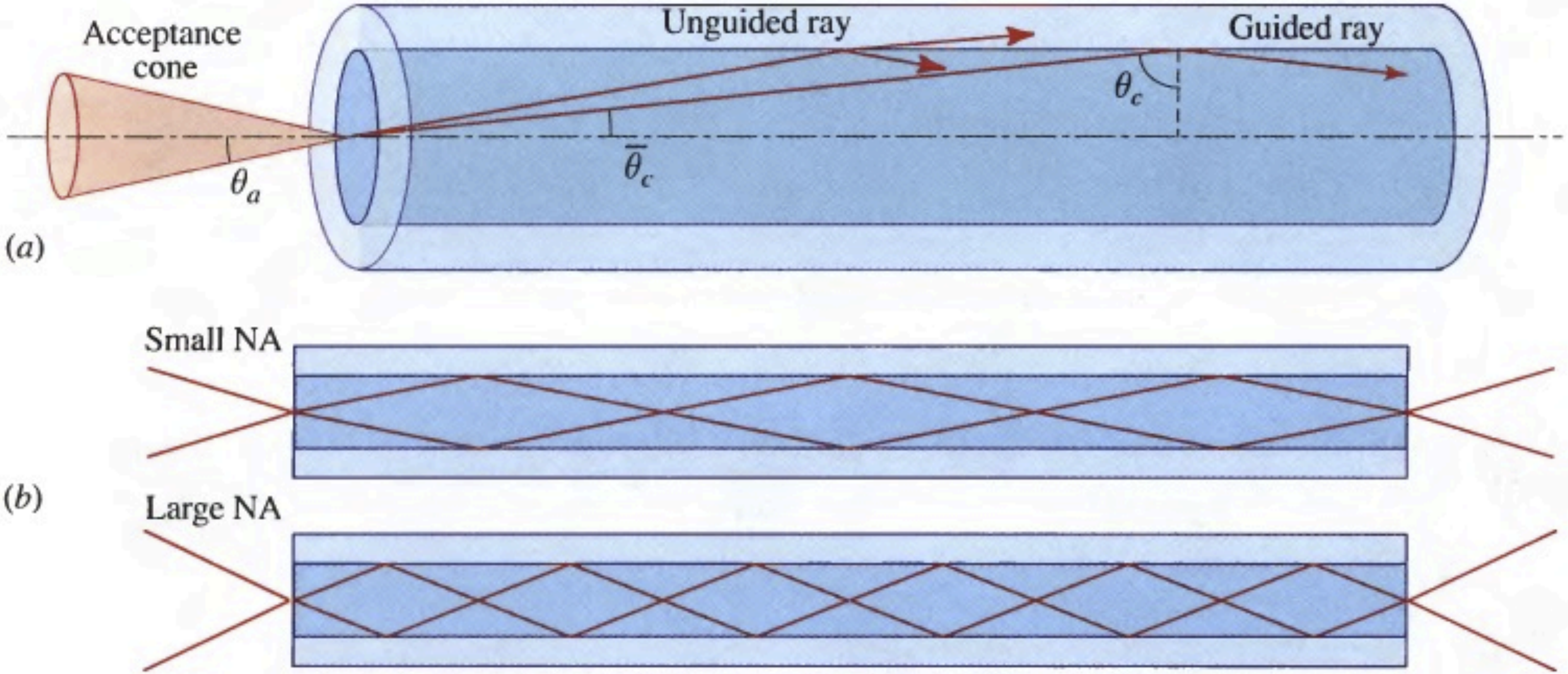

Figure 9.1-3 (*a*) The acceptance angle θ_a of a fiber. Rays within the acceptance cone are guided by total internal reflection. The numerical aperture $\mathrm{NA} = \sin\theta_a$. The angles θ_a and $\overline{\theta}_c$ are typically quite small; they are exaggerated here for clarity. (*b*) The light-gathering capacity of a large NA fiber is greater than that of a small NA fiber.

L'*apertura numerica*

L'**apertura numerica** in ottica è un parametro, un numero puro che indica il massimo angolo utile al sistema (obiettivo, condensatore ottico o altro) per ricevere o emettere luce. La definizione precisa è differente nelle varie branche della materia come microscopia, fibre ottiche, ottica dei laser.

$$\frac{\sin i}{\sin\theta} = \frac{n_1}{n_0}$$

$$\sin\phi(=\cos\theta) > \frac{n_2}{n_1}$$ (riflessione totale interna)

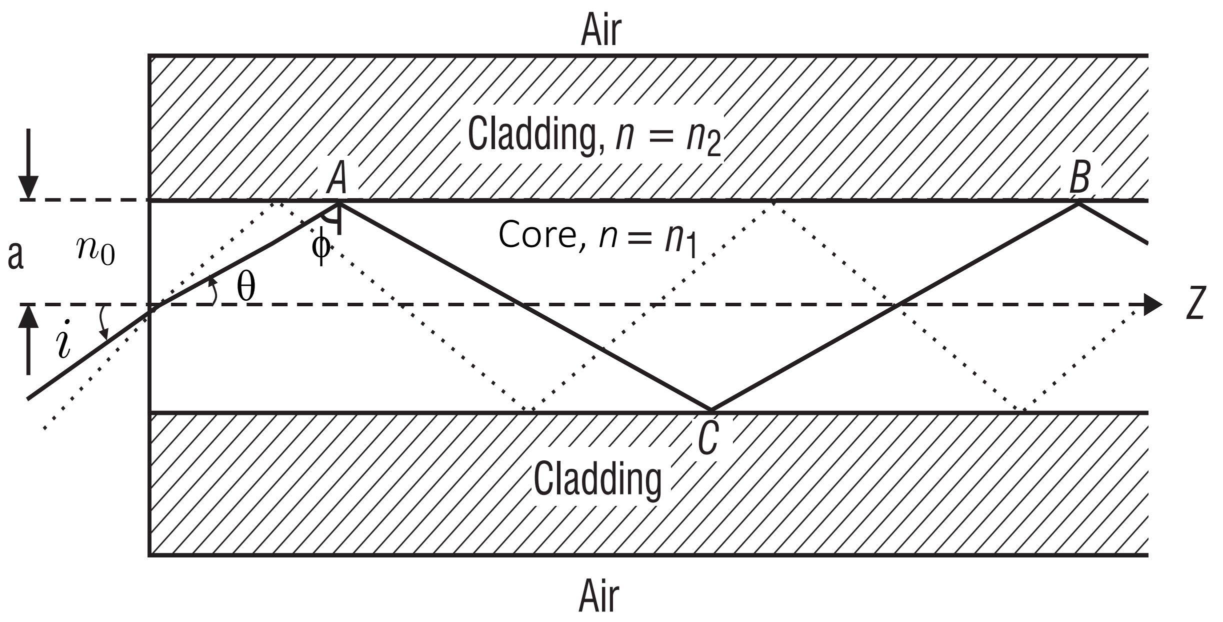

$$\sin\theta < \left[1 - \left(\frac{n_2}{n_1}\right)^2\right]^{1/2}$$

$$\sin i < \frac{n_1}{n_0}\left[1 - \left(\frac{n_2}{n_1}\right)^2\right]^{1/2} \approx \sqrt{n_1^2 - n_2^2} = n_1\sqrt{2\Delta}$$

$$\sin i < \frac{n_1}{n_0}\left[1 - \left(\frac{n_2}{n_1}\right)^2\right]^{1/2} \approx \sqrt{n_1^2 - n_2^2} = n_1\sqrt{2\Delta}$$

$$\mathrm{NA} = \arcsin(\max \sin i) = \arcsin n_1\sqrt{2\Delta}$$

For a typical step-index (multimode) fiber with $n_1 \approx 1.45$ and $\Delta \approx 0.01$, we get

$$\boxed{\sin i_m = n_1\sqrt{2\Delta} = 1.45\sqrt{2 \times (0.01)} = 0.205}$$

so that $i_m \approx 12°$. Thus, all light entering the fiber must be within a cone of half-angle 12°.

Attenuazione nelle fibre ottiche

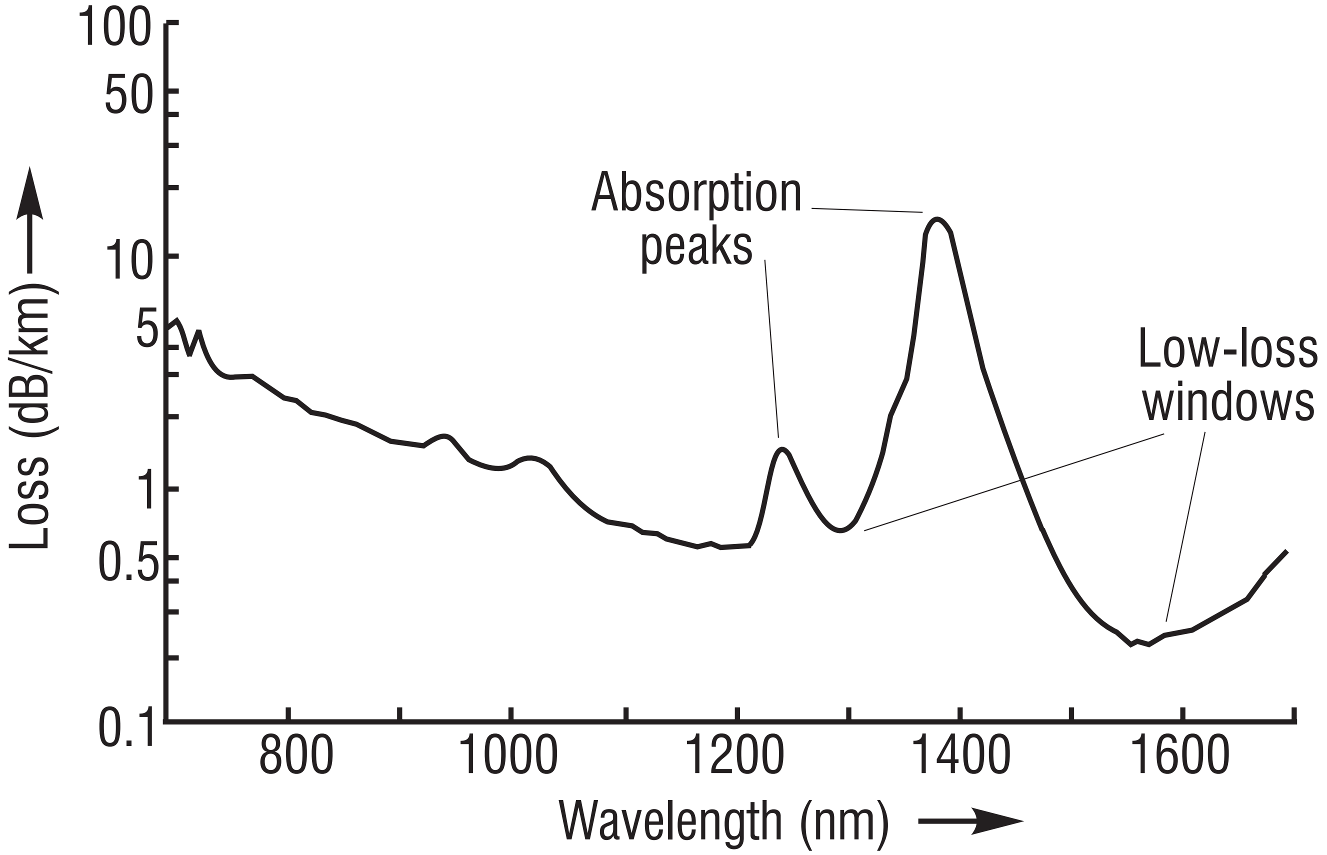

Figure 7-10 *Typical wavelength dependence of attenuation for a silica fiber. Notice that the lowest attenuation occurs at 1550 nm [adapted from Miya, Hasaka, and Miyashita].*

WINDOW GLASS vs OPTICAL FIBER

Glass is the most important component of optical systems. However, common window glass and glass used in photonics applications are worlds apart.

LIGHT TRANSMISSION OF GLASS

How thick can different glass types be so that 1 % of the emitted light is still transmitted?

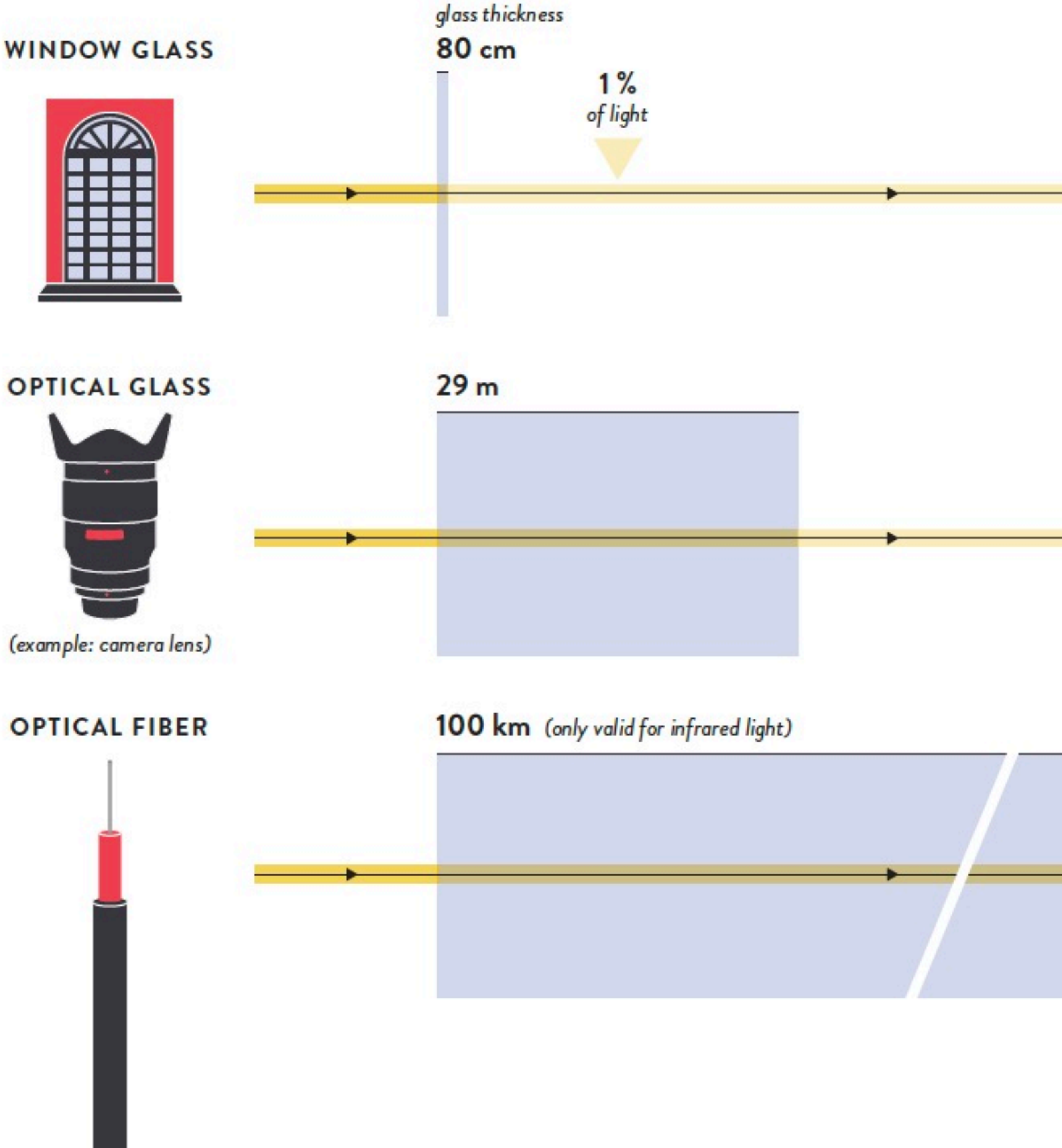

Example 7-3

Calculation of losses using the dB scale become easy. For example, if we have a 40-km fiber link (with a loss of 0.4 dB/km) having 3 connectors in its path and if each connector has a loss of 1.8 dB, the total loss will be the sum of all the losses in dB; or 0.4 dB/km × 40 km + 3 × 1.8 dB = 21.4 dB.

Example 7-4

Let us assume that the input power of a 5-mW laser decreases to 30 μW after traversing through 40 km of an optical fiber. Using Equation 7-12, attenuation of the fiber in dB/km is therefore [10 log (166.7)]/40 ≈ 0.56 dB/km.

Dispersione degli impulsi nelle fibre ottiche

1. Different rays take different times to propagate through a given length of the fiber. We will discuss this for a step-index multimode fiber and for a parabolic-index fiber in this and the following sections. In the language of wave optics, this is known as *intermodal dispersion* because it arises due to different modes traveling with different speeds.[4]
2. Any given light source emits over a range of wavelengths, and, because of the intrinsic property of the material of the fiber, different wavelengths take different amounts of time to propagate along the same path. This is known as *material dispersion* and will be discussed in Section IX.
3. Apart from intermodal and material dispersions, there is yet another mechanism—referred to as *waveguide dispersion* and important only in single-mode fibers. We will briefly discuss this in Section XI.

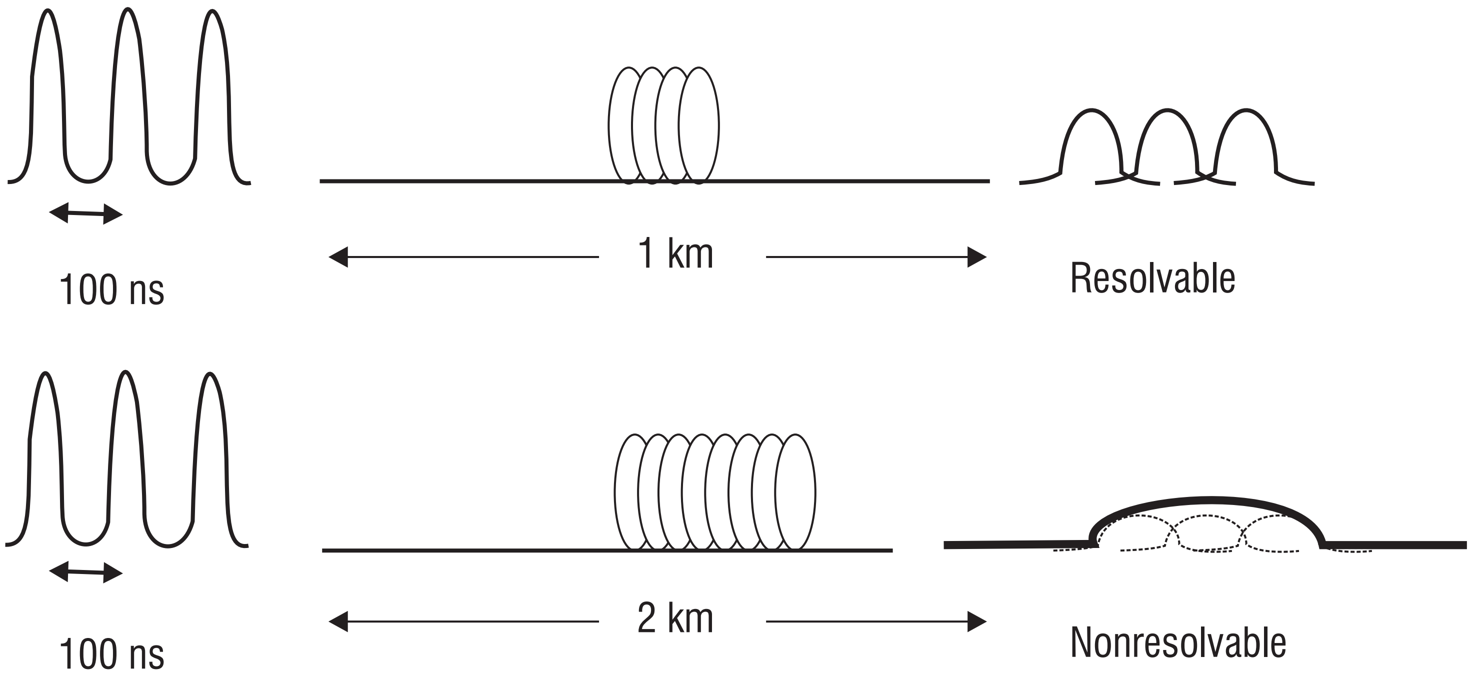

Figure 7-11 *Pulses separated by 100 ns at the input end would be resolvable at the output end of 1 km of the fiber. The same pulses would not be resolvable at the output end of 2 km of the same fiber.*

$$t_{AB} = \frac{AC + CB}{c / n_1} = \frac{AB / \cos\theta}{c / n_1}$$

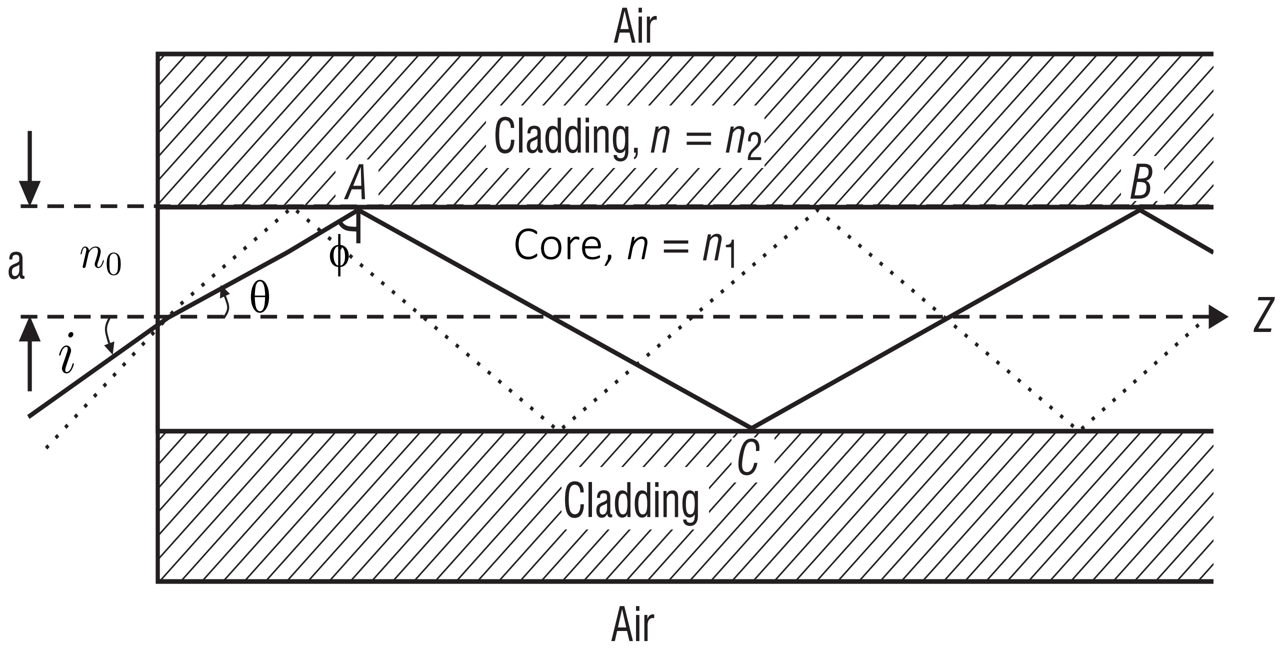

$$t_{AB} = \frac{n_1 AB}{c \cos\theta}$$

$$t_L = \frac{n_1 L}{c \cos\theta}$$ (tempo richiesto per attraversare una lunghezza L di fibra)

$$t_{\min} = \frac{n_1 L}{c}$$ (tempo minimo richiesto, per raggi assiali)

$$t_{\max} = \frac{n_1^2 L}{c n_2}$$ (tempo massimo richiesto, per raggi con $\theta = \theta_c = \cos^{-1}(n_2/n_1)$)

$$\tau_i = t_{max} - t_{min} = \frac{n_1 L}{c}\left[\frac{n_1}{n_2} - 1\right]$$

(intervallo di tempo intermodale)

$$\tau_i \cong \frac{n_1 L}{c}\Delta \approx \frac{L}{2n_1 c}(NA)^2$$

(approssimazione dell'intervallo di tempo intermodale)

$$\tau_2{}^2 = \tau_1{}^2 + \tau_i{}^2$$

(larghezza totale dell'impulso)

larghezza iniziale dell'impulso

For a typical (multimoded) step-index fiber, if we assume $n_1 = 1.5$, $\Delta = 0.01$, $L = 1$ km, we would get

$$\tau_1 = \frac{1.5 \times 1000}{3 \times 10^8} \times 0.01 = 50 \text{ ns/km} \tag{7-20}$$

That is, a pulse traversing through the fiber of length 1 km will be broadened by 50 ns. Thus, two pulses separated by, say, 500 ns at the input end will be quite resolvable at the end of 1 km of the fiber. However, if consecutive pulses were separated by, say, 10 ns at the input end, they would be absolutely unresolvable at the output end. Hence, in a 1-Mbit/s fiber optic system, where we have one pulse every 10^{-6} s, a 50-ns/km dispersion would require repeaters to be placed every 3 to 4 km. On the other hand, in a 1-Gbit/s fiber optic communication system, which requires the transmission of one pulse every 10^{-9} s, a dispersion of 50 ns/km would result in intolerable broadening even within 50 meters or so. This would be highly inefficient and uneconomical from a system point of view.

Fibre con "indice parabolico"

$$n^2(r) = n_1^{\,2}\left[1-2\Delta\left(\frac{r}{a}\right)^2\right] \qquad 0<r<a$$

$$n^2(r) = n_2^2 = n_1^{\,2}(1-2\Delta) \qquad r>a$$

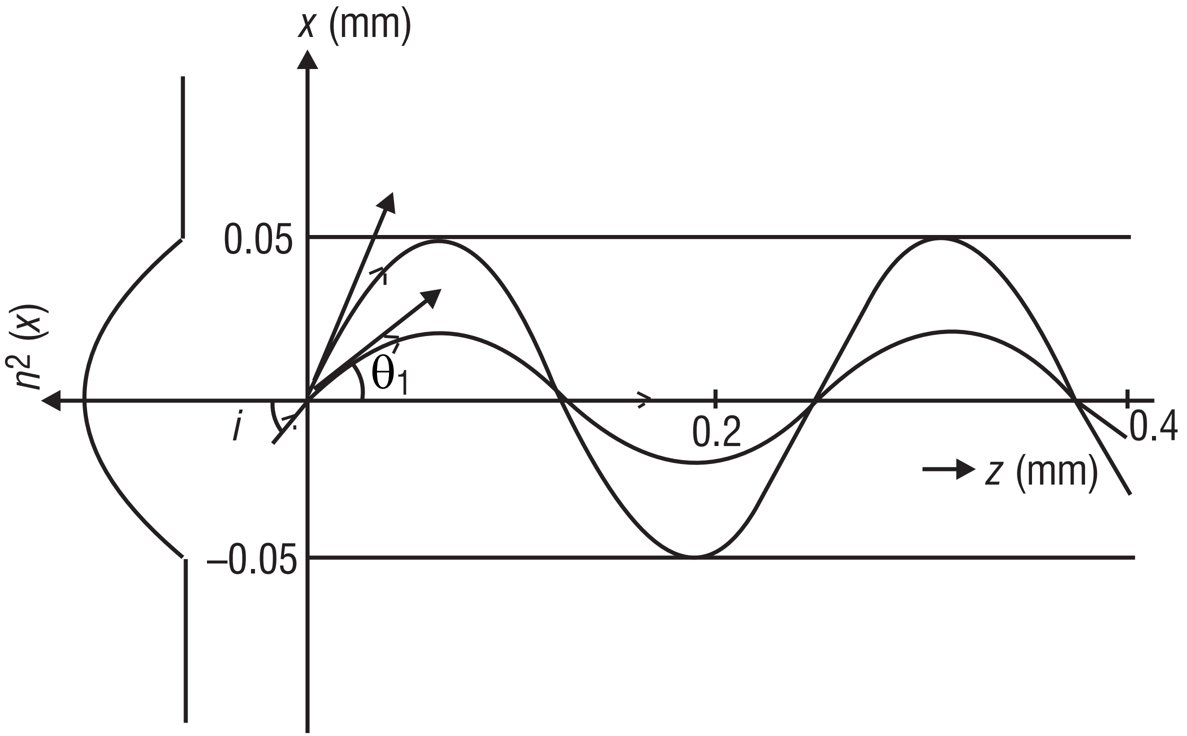

Figure 7-12 *Different ray paths in a parabolic-index fiber*

$$\tau_{\text{im}} = \frac{n_2 L}{2c}\left(\frac{n_1-n_2}{n_2}\right)^2 \approx \frac{n_2 L}{2c}\Delta^2 \approx \frac{L}{8cn_1^{\,3}}(NA)^4$$

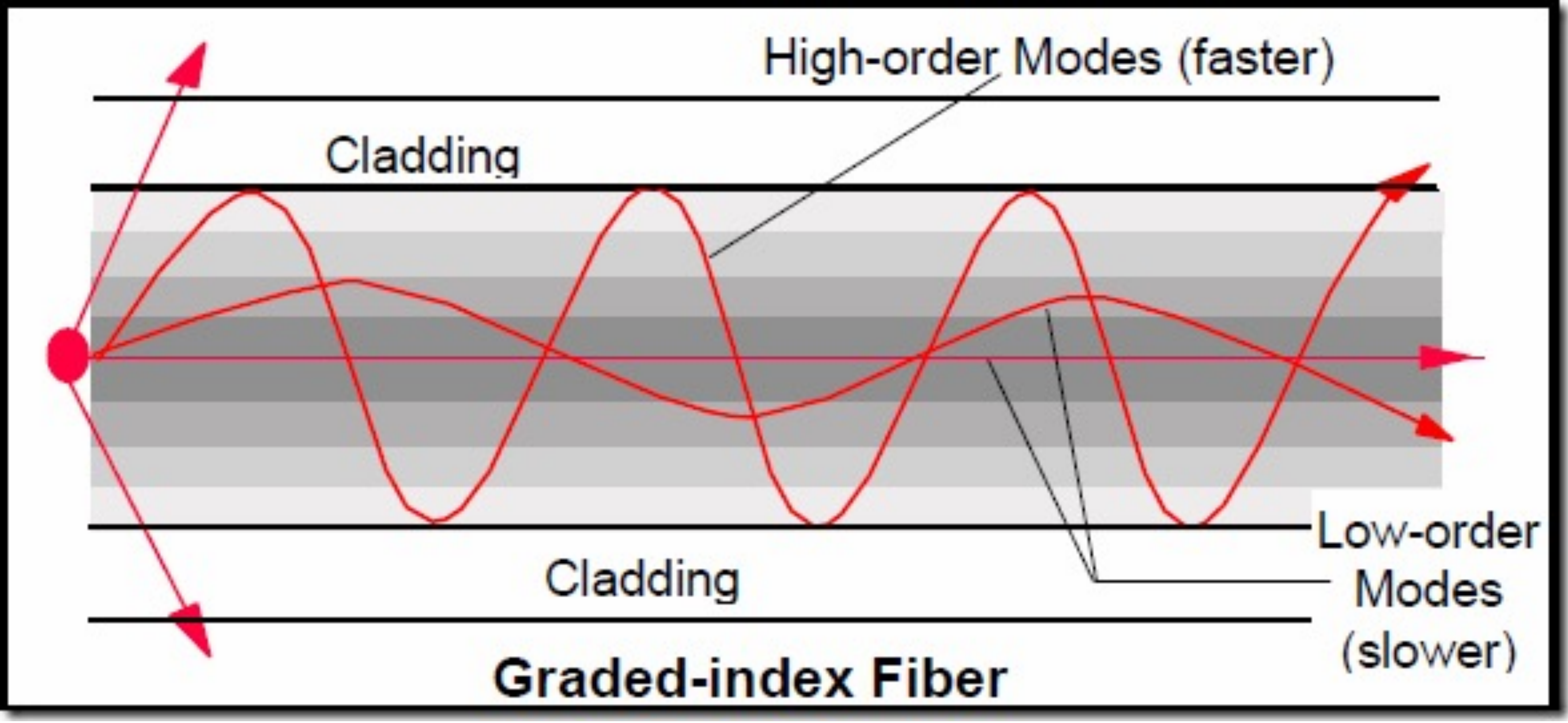
High-order Modes (faster)
Cladding
Cladding
Low-order Modes (slower)
Graded-index Fiber

WINDOW GLASS vs OPTICAL FIBER

Glass is the most important component of optical systems. However, common window glass and glass used in photonics applications are worlds apart.

LIGHT TRANSMISSION OF GLASS

How thick can different glass types be so that 1 % of the emitted light is still transmitted?

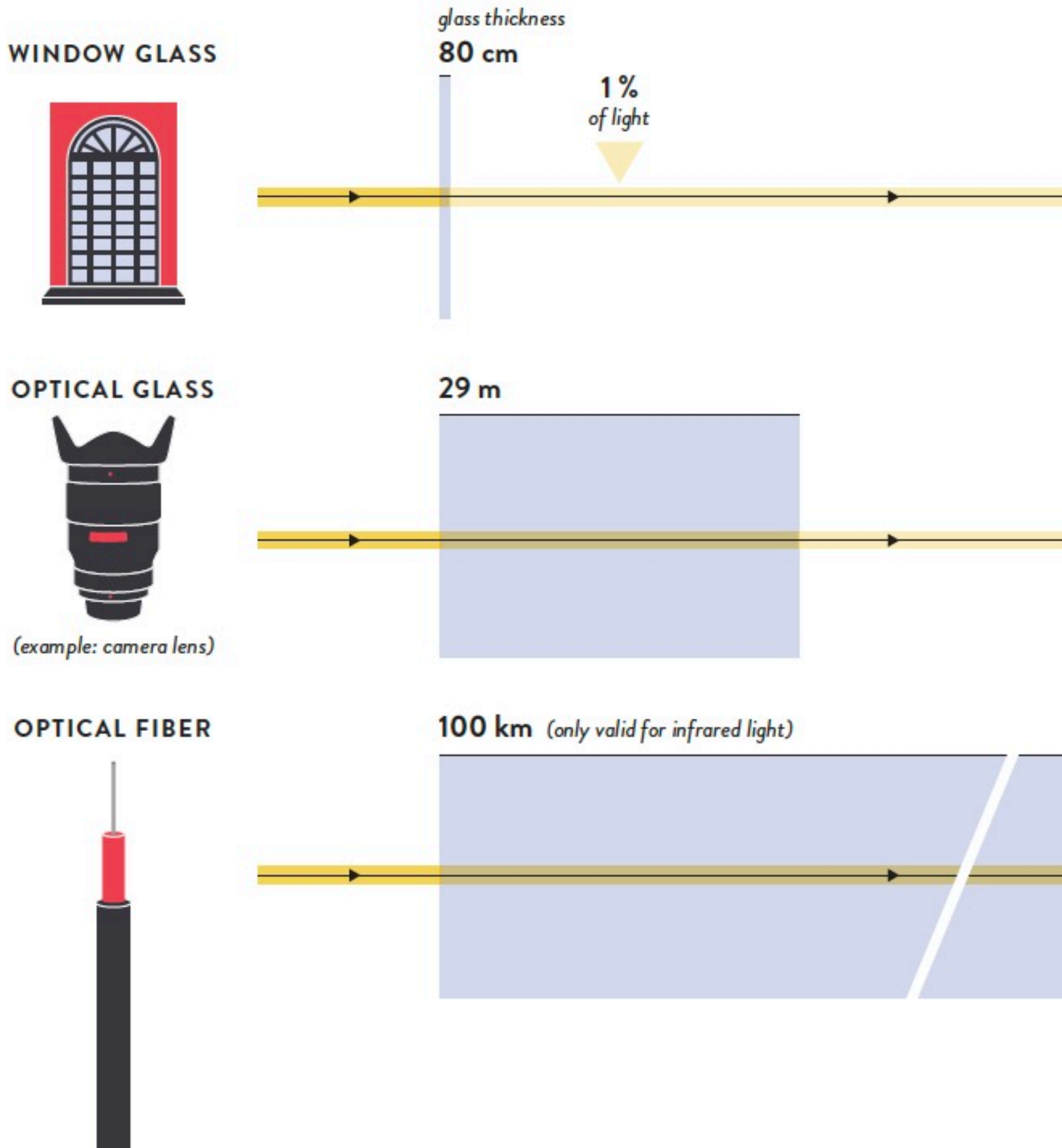

Dozens of data signals can be coupled into one single optical fiber and be separated again at the receiver's end. The signals can be very finely distinguished based on their wavelength (spectral color), polarization, and phase.

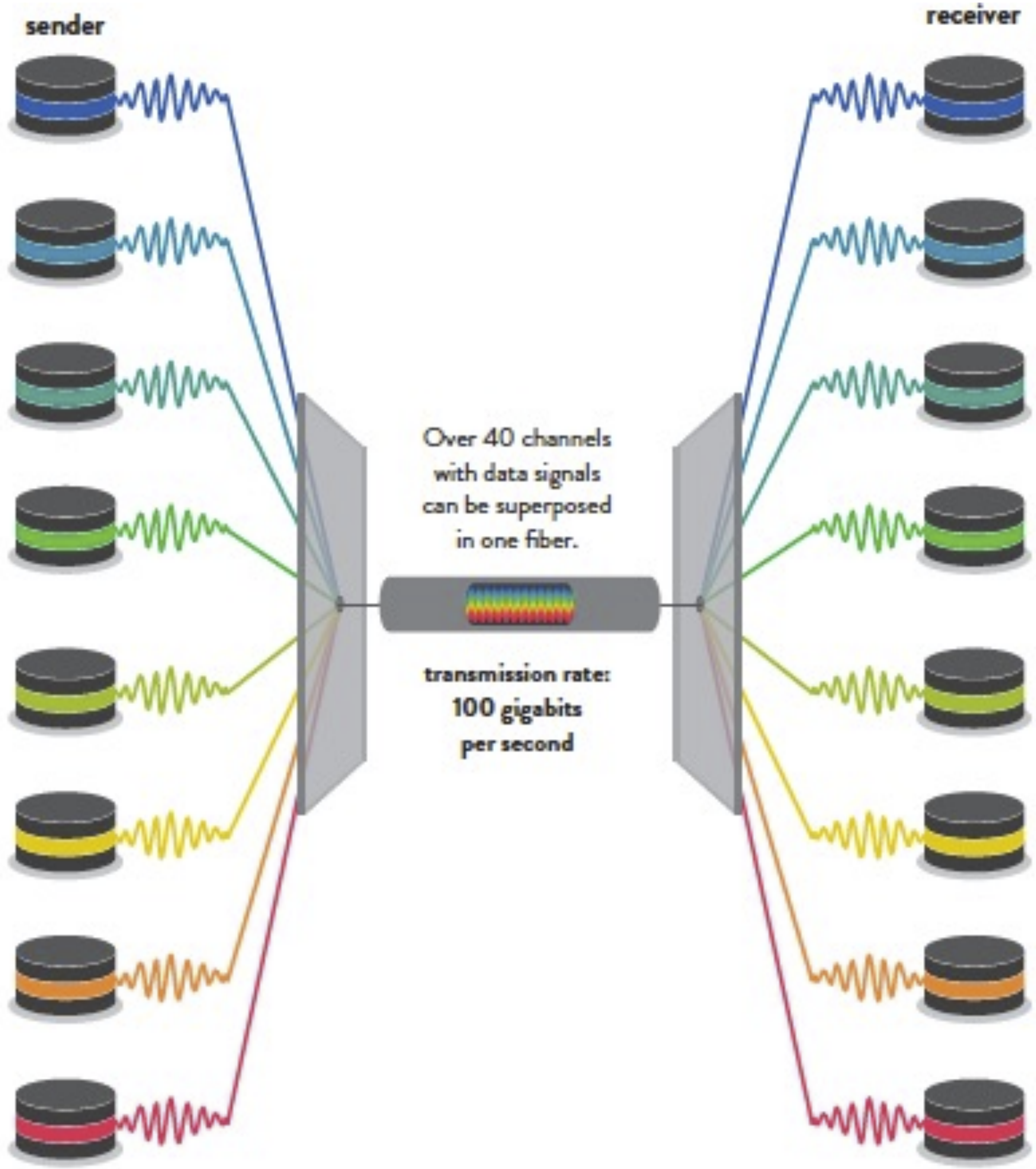

In 1988, the first transatlantic optical fiber cable, the TAT-8, went into operation. Optical fiber quickly replaced copper cables to meet the fast-growing need for greater capacity. Today, submarine cables with capacities of up to several terabytes per second connect the whole Earth.

Optical fibers offer substantially higher transmission rates, while simultaneously providing large ranges. Other advantages are lighter cables, lower space requirements, and fewer repeaters. The operation and maintenance costs are also significantly reduced.

Data cable in city area

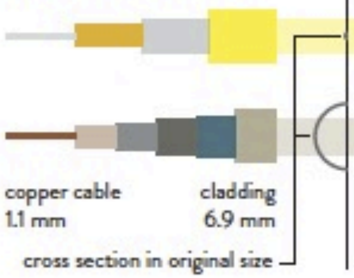

	transfer speed in Mbit/s	range in km, without repeater	shelf life in years	weight 100 m cable in kg	energy consumption in watts per user
optical fiber cable	1000	100	50	0.6	2
copper cable	50	2	5	5.8	10

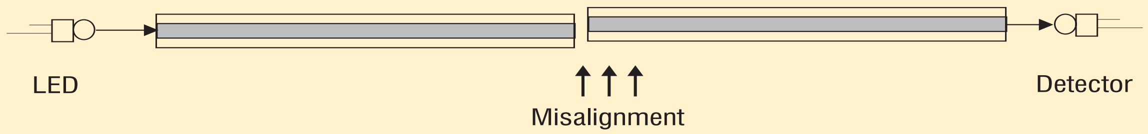

Figure 7-18 *A change in the transverse alignment between two fibers changes the coupling and hence the power falling on the detector.*

OPTICS LETTERS / Vol. 5, No. 1 / January 1980

Moving fiber-optic hydrophone

W. B. Spillman, Jr., and R. L. Gravel

Sperry Research Center, Sudbury, Massachusetts 01776

Received September 24, 1979

A fiber-optic hydrophone based on an intensity-modulation mechanism is described. The device possesses sufficient sensitivity to detect typical deep-sea noise levels in the frequency range 100 Hz to 1 kHz and to detect static displacements of 8.3×10^{-3} Å. It is not susceptible to phase noise and is insensitive to static-pressure head variations. The hydrophone is passive in nature and requires no electrical power. Ease of fabrication and potential low cost make this device an attractive candidate for incorporation into practical fiber-optic acoustic sensing arrays.

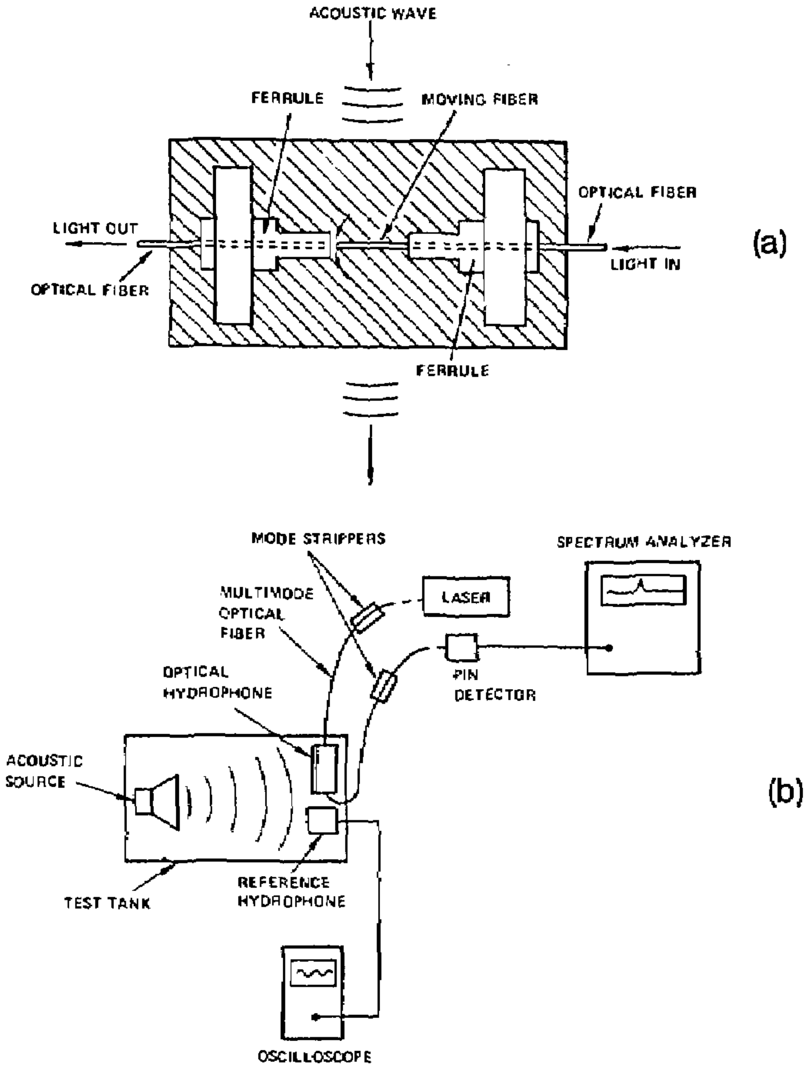

Fig. 1. Moving-fiber optical hydrophone: (a) device configuration, (b) experimental setup.

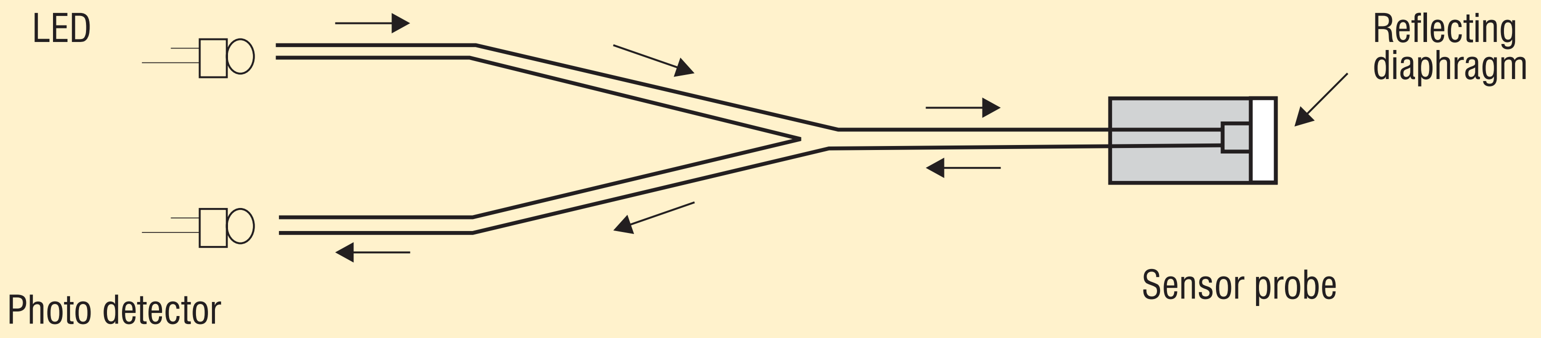

Figure 7-19 *Light returning to the detector changes as the shape of the reflecting diaphragm changes due to changes in external pressure.*

Single Sensors

newLight FS62

Fiber Bragg Grating (FBG) based sensors for stable and accurate strain measurements.

newLight FS63

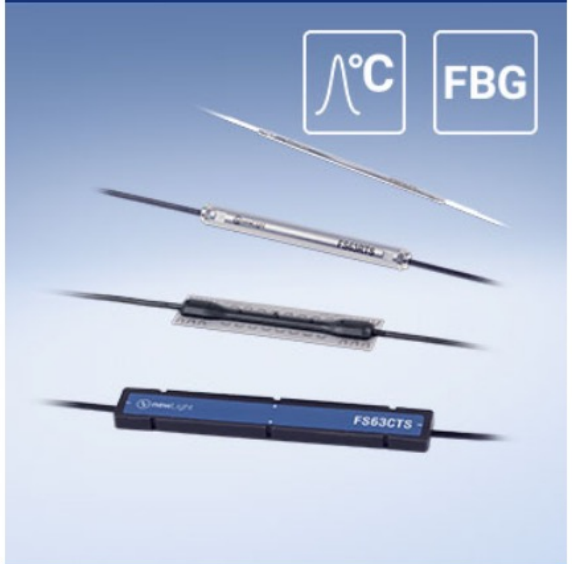

Fiber Bragg Grating (FBG) based temperature sensors. Accurate and clean temperature measurements for thermal mapping or

newLight FS64

Sensor to measure small inclination variations. It uses two Fiber Bragg Gratings (FBG) in a push-pull configuration for effective

newLight FS65

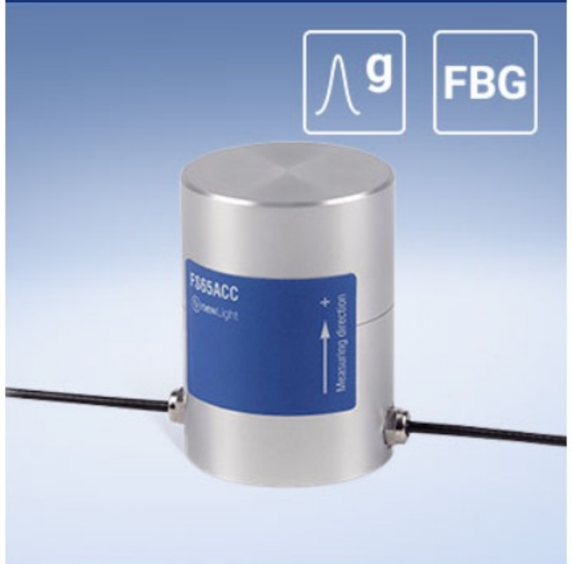

Fiber Bragg Grating (FBG) based accelerometer for vibration measurements under low frequencies.

Sensor Groups

newLight FS70

Several Fiber Bragg Gratings (FBGs) on the same fiber suited for multi point measurements of strain in laboratories and other optical applications

newLight FS76

Arrays of strain and temperature sensors pre-assembled to the same cable for efficient installation.

Guide d'onda ottiche

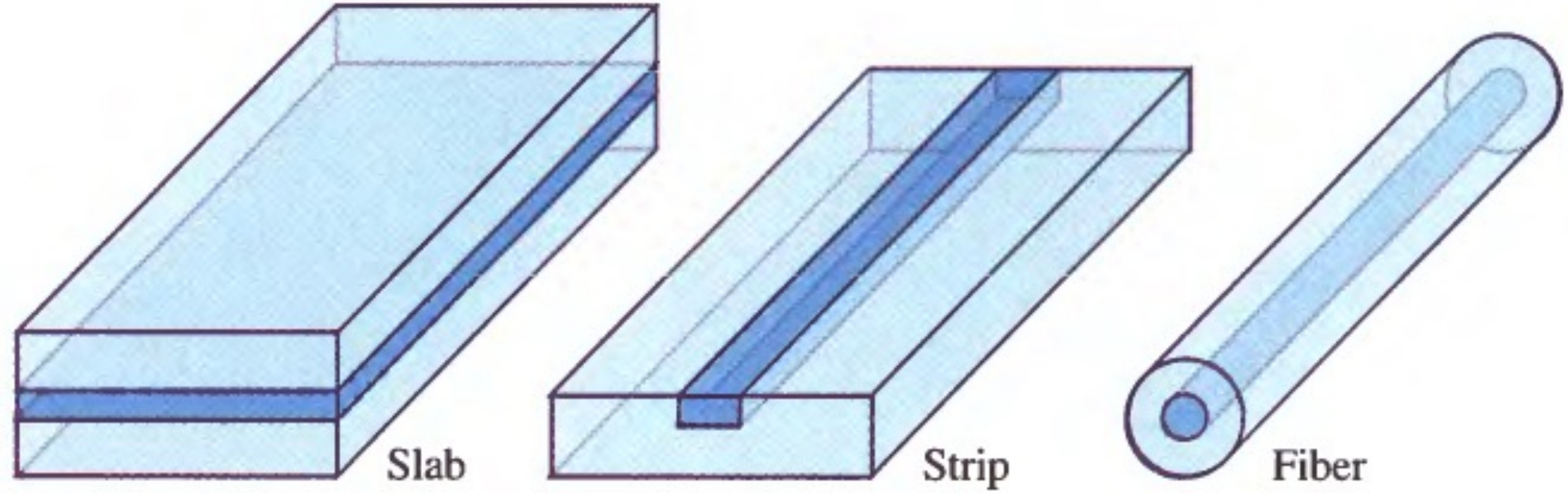

(figure from Saleh & Teich, Photonics, 2nd ed., 2007)

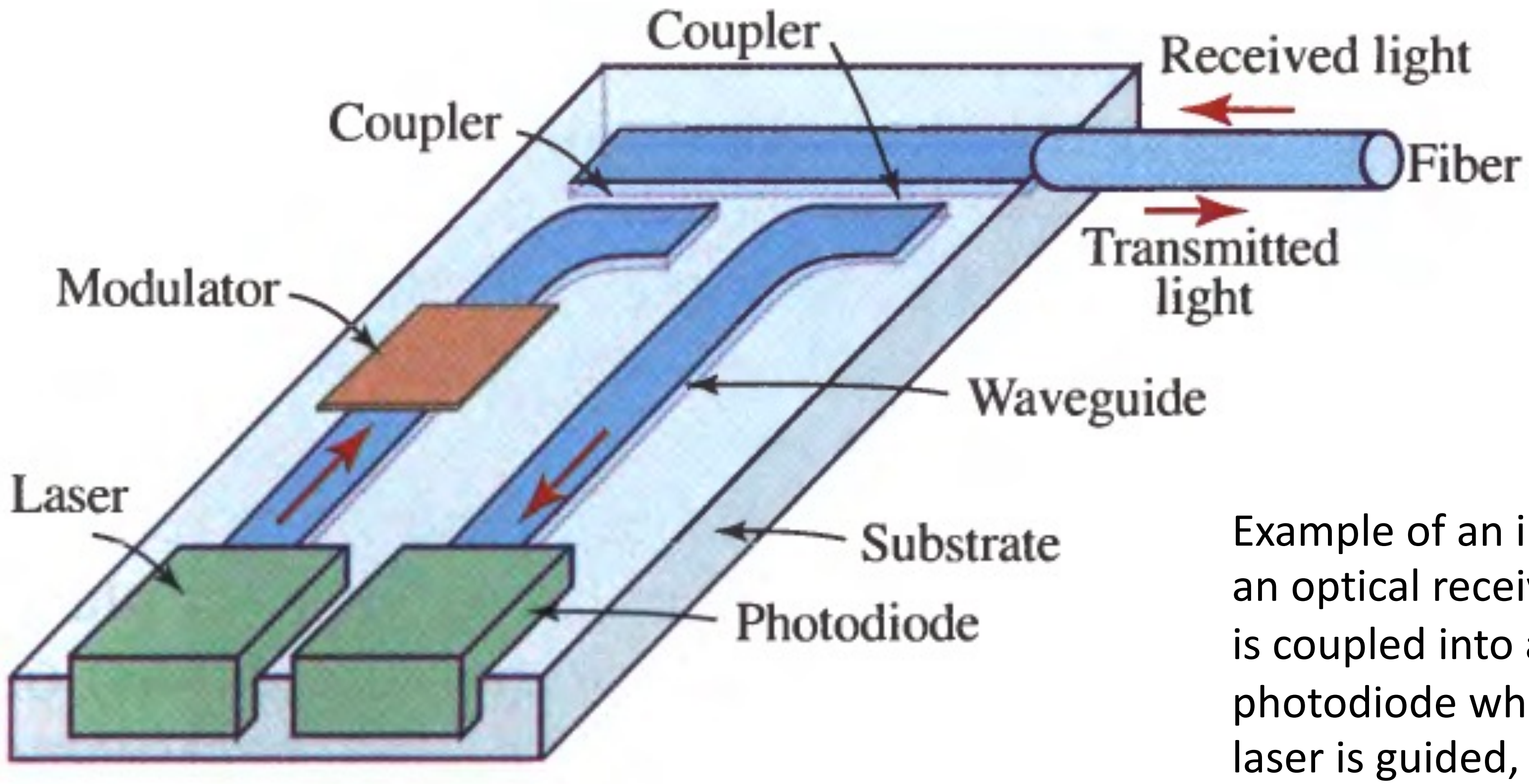

Example of an integrated-optic device used as an optical receiver/transmitter. Received light is coupled into a waveguide and directed to a photodiode where it is detected. Light from a laser is guided, modulated, and coupled into a fiber for transmission.

(taken from Saleh & Teich, Photonics, 2nd ed., 2007)

Una coppia di specchi piani e paralleli come guida d'onda planare

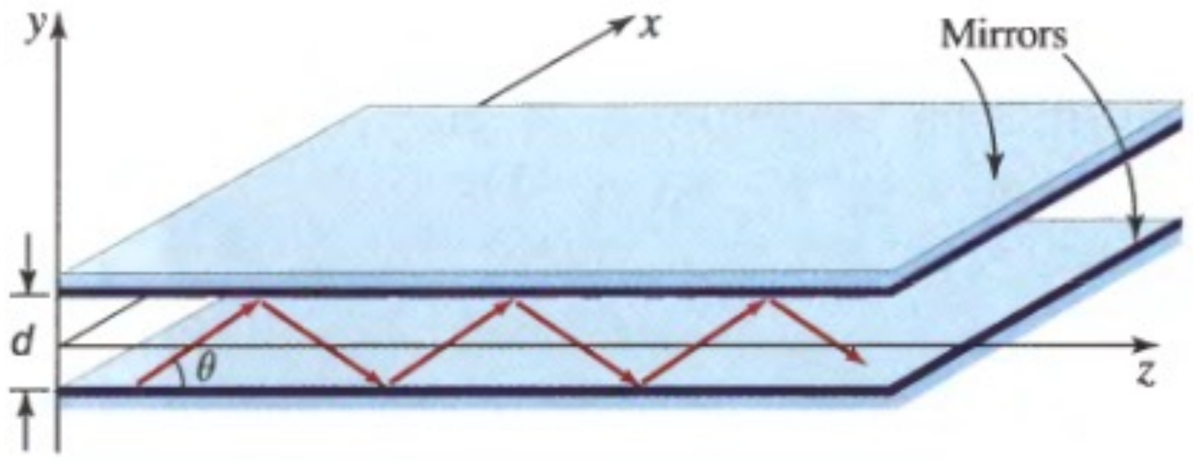

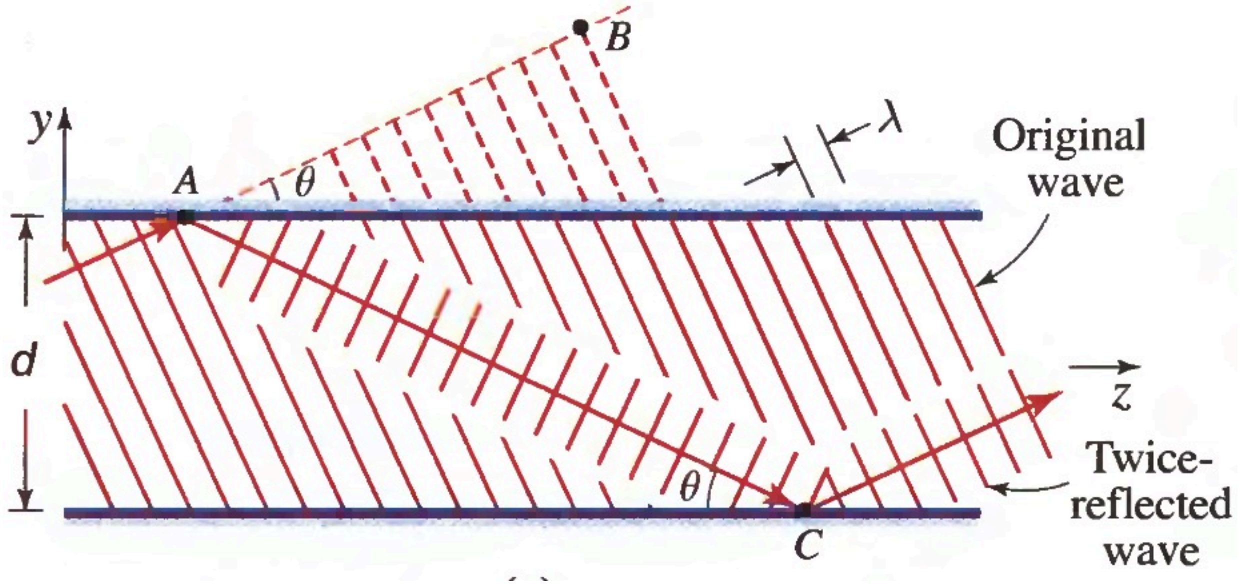

Somma coerente tra i campi dell'onda iniziale e quella riflessa due volte: le creste "si sommano", non ci sono situazioni in cui c'è interferenza distruttiva.

Questa condizione corrisponde solo a certi angoli di propagazione, e corrisponde ai *modi propri* della radiazione nella guida d'onda.

Il mezzo che costituisce la guida d'onda ha indice di rifrazione *n*, quindi:

$$c = \frac{c_v}{n}; \quad k = nk_v; \quad \lambda = \frac{\lambda_v}{n}$$

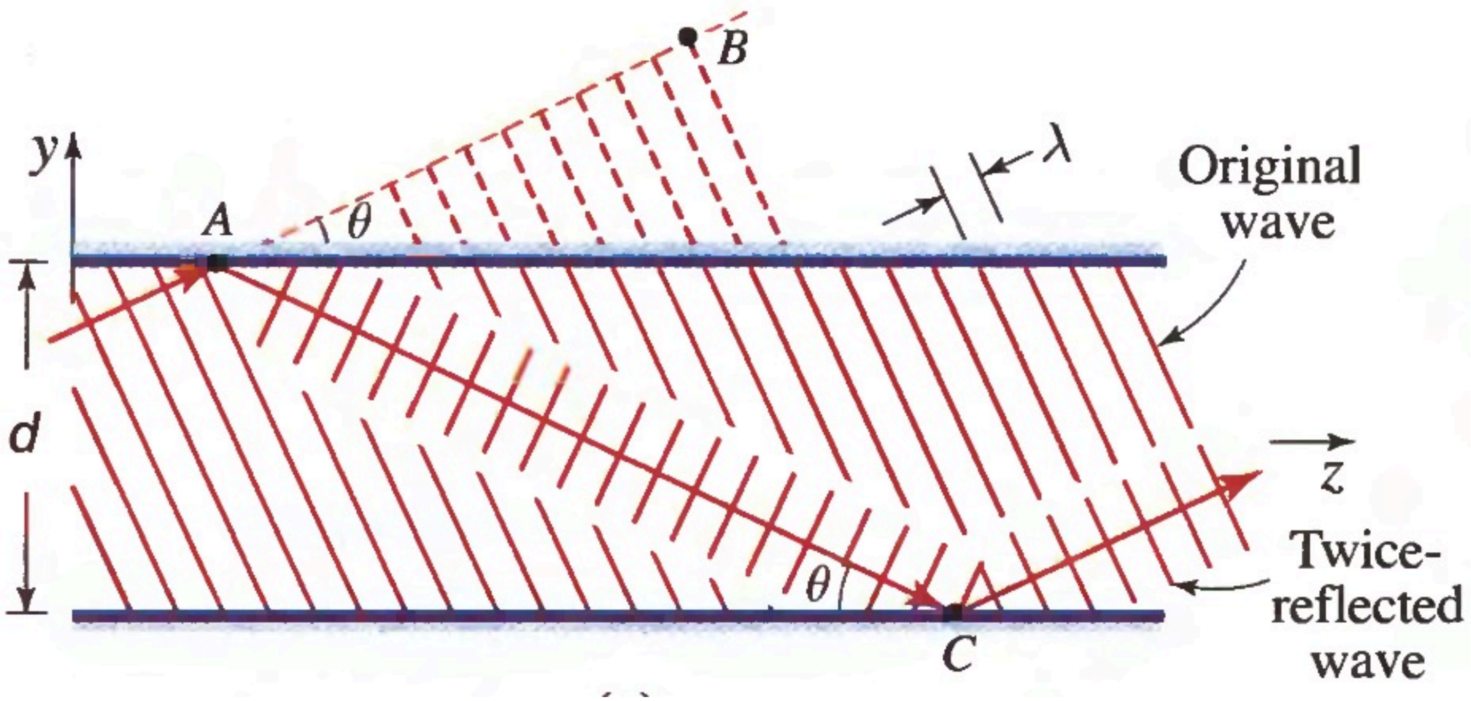

La periodicità dei modi propri richiede che sia AB, sia AC siano multipli della lunghezza d'onda, quindi

$$\overline{AC} = \frac{d}{\sin\theta}; \quad \overline{AB} = \frac{d}{\sin\theta}\cos 2\theta$$

$$\overline{AC} - \overline{AB} = m\lambda$$

$$\sin\theta_m = m\frac{\lambda}{2d}$$

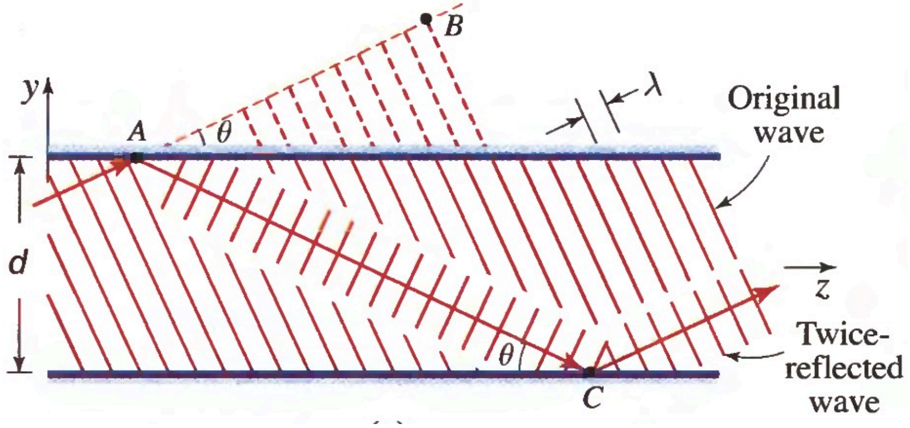

Il numero d'onda trasverso è la proiezione del numero d'onda nella direzione trasversa rispetto l'asse z. Troviamo quindi

$$k_{t,m} = k \times \sin\theta_m = \frac{2\pi}{\lambda} \times m\frac{\lambda}{2d} = m\frac{\pi}{d}$$

Analogamente, il numero d'onda in direzione longitudinale (costante di propagazione) è dato da

$$\beta_m^2 = k^2 - k_{t,m}^2 = k^2 - \frac{m^2\pi^2}{d^2}$$

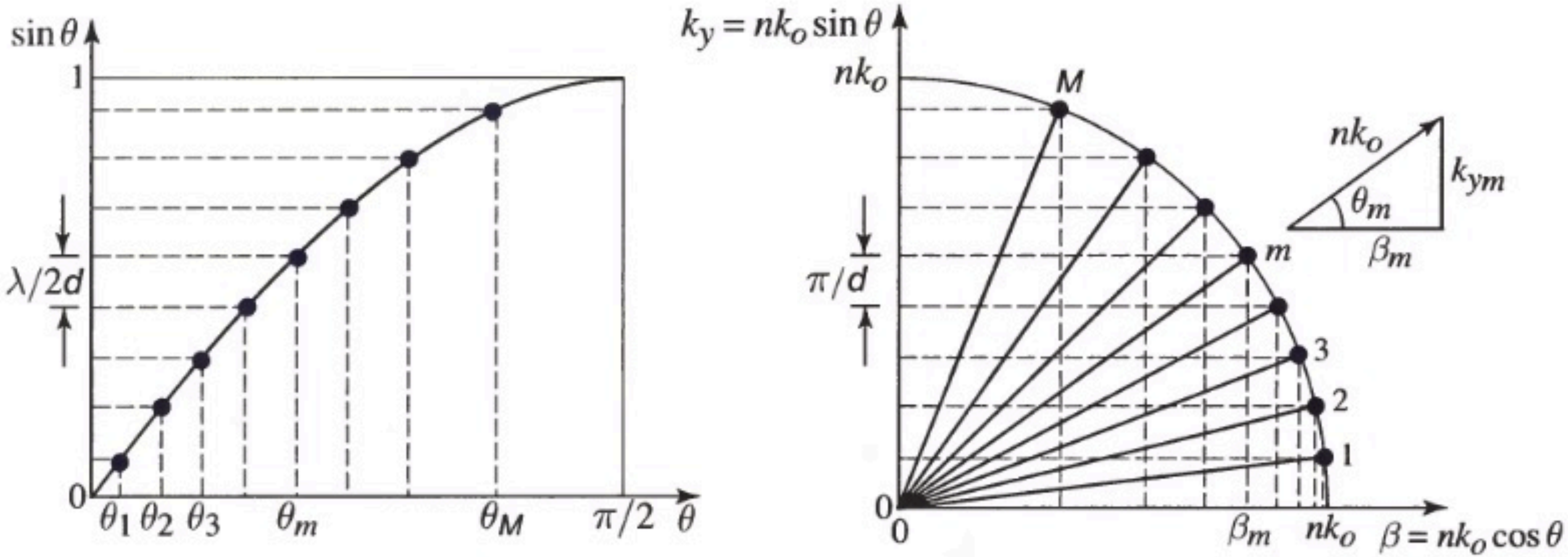

Figure 8.1-3 The bounce angles θ_m and the wavevector components of the modes of a planar-mirror waveguide (indicated by dots). The transverse components $k_{ym} = k \sin\theta_m$ are spaced uniformly at multiples of π/d, but the bounce angles θ_m and the propagation constants β_m are not equally spaced. Mode $m = 1$ has the smallest bounce angle and the largest propagation constant.

Distribuzione di campo elettrico

Campo con numero d'onda trasverso verso l'alto

$$A_m \exp(-ik_t y - i\beta_m z)$$

Campo con numero d'onda trasverso verso il basso (deve essere opportunamente sfasato, si cerchi di capire perché)

$$e^{i(m-1)\pi} A_m \exp(ik_t y - i\beta_m z)$$

Campo risultante

$$\begin{aligned} E_x(y,z) &= A_m \exp(-ik_t y - i\beta_m z) + e^{i(m-1)\pi} A_m \exp(ik_t y - i\beta_m z) \\ &= a_m u_m(y) \exp(-i\beta_m z) \end{aligned}$$

dove $u_m(y) = \begin{cases} \sqrt{\dfrac{2}{d}} \cos \dfrac{m\pi y}{d} & m \text{ dispari} \\ \sqrt{\dfrac{2}{d}} \sin \dfrac{m\pi y}{d} & m \text{ pari} \end{cases}$ e $a_m = \begin{cases} \sqrt{2d} A_m & m \text{ dispari} \\ i\sqrt{2d} A_m & m \text{ pari} \end{cases}$

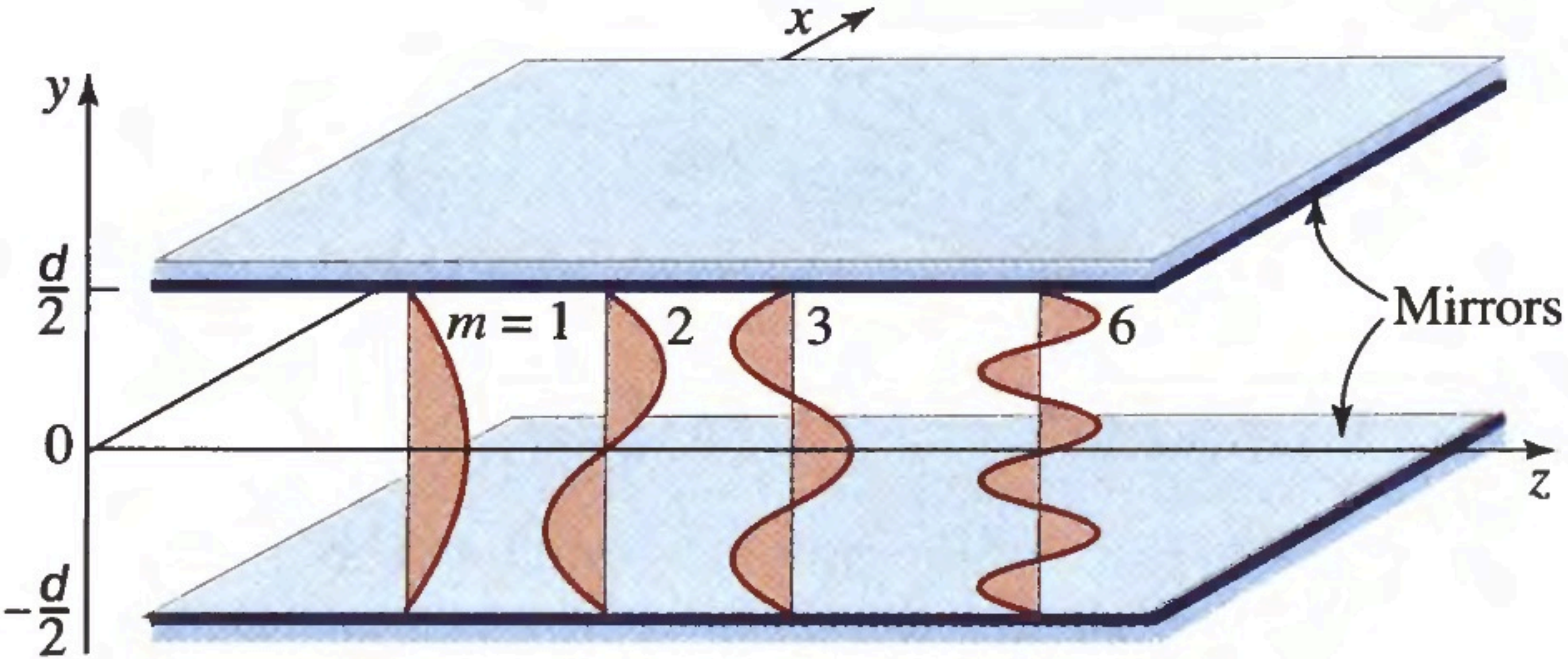

x
y
$\frac{d}{2}$
0
$-\frac{d}{2}$
$m = 1$
2
3
6
Mirrors
z

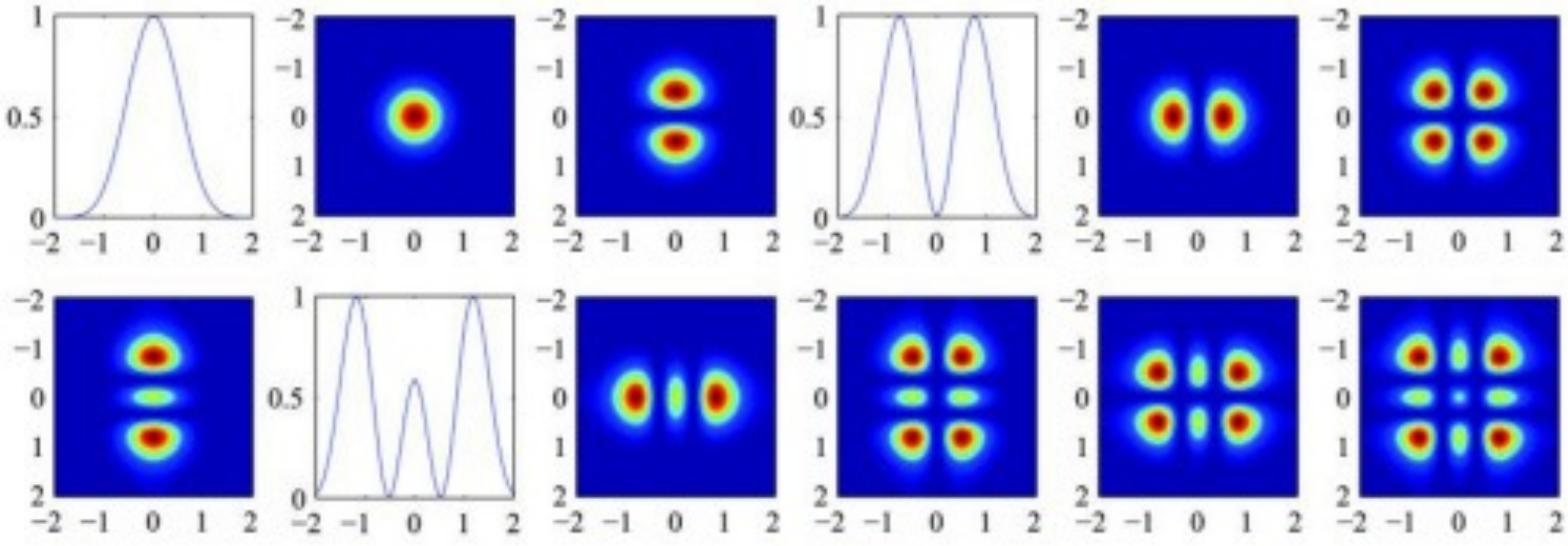

Esempio di modi in una cavità risonante (caso speciale di guida d'onda)

Numero di modi

$$\sin\theta_m = m\frac{\lambda}{2d} \leq 1 \quad \Rightarrow \quad m \leq \frac{2d}{\lambda}$$

$$M = \max m = \left\lfloor \frac{2d}{\lambda} \right\rfloor$$

se M = 0 allora la guida d'onda non riesce a trasportare alcun modo di propagazione. Si noti anche che la lunghezza d'onda massima perché ci sia almeno un modo è data da

$$\frac{2d}{\lambda_c} = 1 \quad \Rightarrow \quad \lambda \leq \lambda_c = 2d \qquad \omega_c = \frac{2\pi c}{\lambda_c}$$

lunghezza d'onda di taglio

frequenza di taglio

Relazione di dispersione

$$\omega = ck$$

relazione di dispersione nel vuoto

$$\beta_m^2 = (\omega/c)^2 - m^2\pi^2/d^2$$

relazione di dispersione in fibra

$$\beta_m = \frac{\omega}{c}\sqrt{1 - m^2\frac{\omega_c^2}{\omega^2}}$$

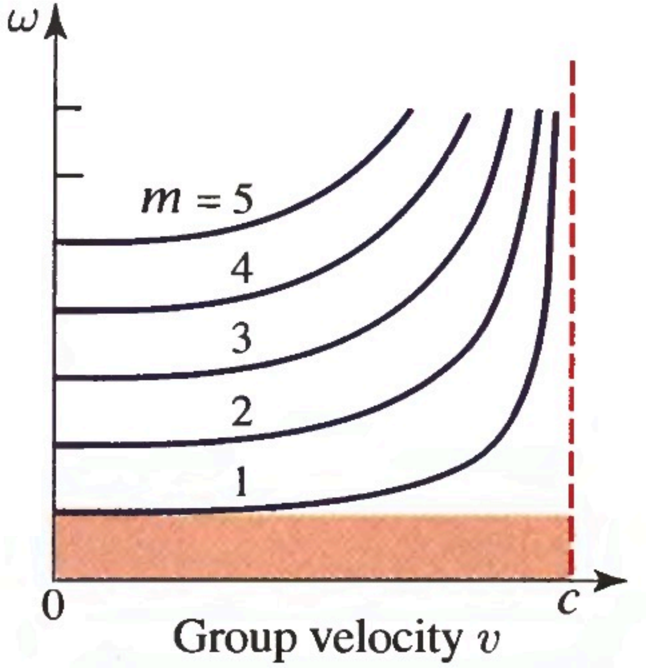

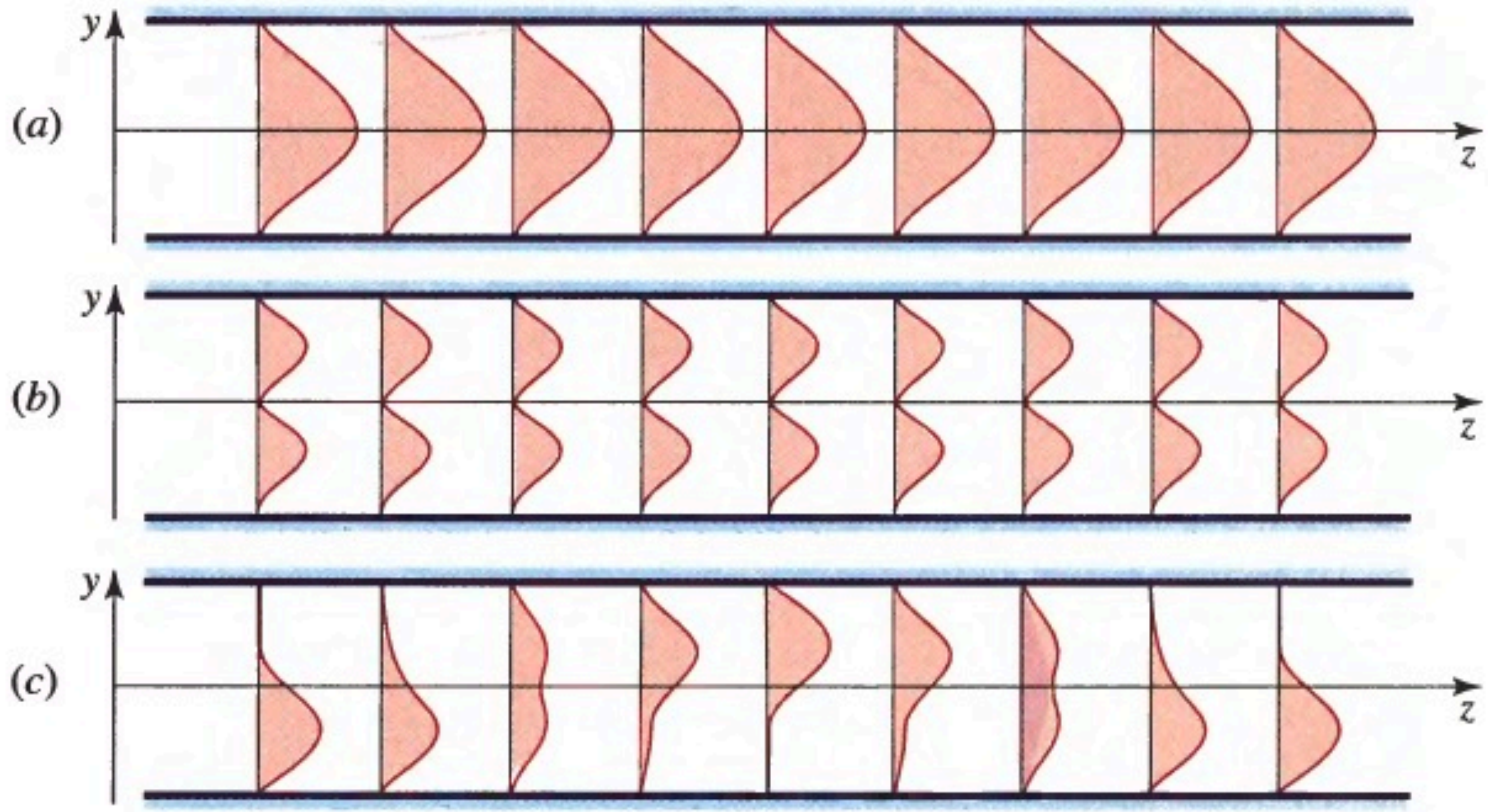

Figure 8.1-8 Variation of the intensity distribution in the transverse direction y at different axial distances z. (a) The electric-field complex amplitude in mode 1 is $E(y, z) = u_1(y) \exp(-j\beta_1 z)$, where $u_1(y) = \sqrt{2/d} \cos(\pi y/d)$. The intensity does not vary with z. (b) The complex amplitude in mode 2 is $E(y, z) = u_2(y) \exp(-j\beta_2 z)$, where $u_2(y) = \sqrt{2/d} \sin(2\pi y/d)$. The intensity does not vary with z. (c) The complex amplitude in a mixture of modes 1 and 2, $E(y, z) = u_1(y) \exp(-j\beta_1 z) + u_2(y) \exp(-j\beta_2 z)$. Since $\beta_1 \neq \beta_2$, the intensity distribution changes with z.